

Research Article

Non-force electromagnetic fields in nature and experiments on earth: Part 2

VV Aksenov*

Institute of Computational Mathematics and Mathematics, Geophysics of Siberian Branch of Russian Academy of Sciences, Lavrentieva Avenue, 6, Novosibirsk, 630090, Russian Federation

More Information

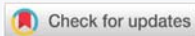
***Address for Correspondence:** VV Aksenov, Institute of Computational Mathematics and Mathematics Geophysics of Siberian Branch of Russian Academy of Sciences, Lavrentieva Avenue, 6, Novosibirsk, 630090, Russian Federation, Tel: +7 913 786 83 21; Email: Aksenov@omzg.sgcc.ru

Submitted: 13 May 2020; **Approved:** 08 July 2020; **Published:** 13 July 2020

How to cite this article: Aksenov VV. Non-force electromagnetic fields in nature and experiments on earth: Part 2. Int J Phys Res Appl. 2020; 3: 075-114.

DOI: 10.29328/journal.ijpra.1001026

Copyright: © 2020 Aksenov VV. This is an open access article distributed under the Creative Commons Attribution License, which permits unrestricted use, distribution, and reproduction in any medium, provided the original work is properly cited.



Introduction

The manifestation of non-force electromagnetic fields in nature and in experiments on Earth is interesting and important in the part that would confirm the numerous physical models that have been calculated and presented in the scientific literature [5,6,15,17].

It should be noted that the theoretical modeling of non-force electromagnetic fields on Earth almost completely goes back to the ideology developed by Yu. Parker [5] for cosmic magnetic fields.

Attempts to experimentally reproduce non-force magnetic fields on Earth based on the ideology of Yu. Parker do not lead to success, from our point of view, because there is too much difference in the similarity criteria of the Reynolds magnetic number ($Re_m = L\sigma\mu|V| = L$) in space ($Re_m \sim 10^{17}$) and on Earth (no more than $Re_m \sim 10^5$). This difference, from our point of view, closes the way to success for numerous theories of Dynamo excitation of the magnetic field on Earth. These theories were never able to reproduce the observed data from the two international geophysical years 1933 and 1957/58 and the world magnetic survey 1964/65. Although it should be noted their visual appeal in the image of the source of the main geomagnetic field on Earth.

The author, having considered the basics of the methods proposed by Yu. Parker for excitation and maintenance of the magnetic field in Space concluded that these methods are unacceptable for the Earth. This led to the formulation and proof of the author's theorem on the source of a non-strong magnetic field on the Earth, published in the first part of the article [50].

According to this theorem, the natural electromagnetic field on Earth is excited by spherical toroidal electric currents that take place in the Earth's core and in the ionosphere, (the variable part is variations).

The theory of new electrodynamics of toroidal currents is developed in sufficient detail by the author [10,50]. Its application to experiments on Earth is given in this article.



Natural sources of the Earth's non-force magnetic and electric fields

Since the time of prediction of non-force magnetic fields [1], a large number of theoretical studies have been carried out [5,6], and [15] to investigate the versions of magnetic fields, whose configuration of force lines was turbulently "twisting" in an odd manner. Such a way of investigation brought about the appearance of toroidal non-force magnetic fields. However, experiments on the Earth aimed at obtaining a non-force magnetic field based on the turbulence of the initial magnetic field did not yield a positive result [30]. In our opinion, this is associated with small Reynolds Re_m numbers for the Earth due to a small characteristic size of L in its definition (Section 1, [50]).

In the technical physics, it appeared possible to obtain non-force electromagnetic fields on the Earth only based on Theorem 4 [50] affirming that spherical toroidal components of the current density and that only these components simultaneously generate toroidal non-force and poloidal force magnetic fields.

Therefore, there arises a problem of experimental detection of toroidal non-force magnetic fields in the Earth's magnetic field. According to Theorem 4 [50], the author has developed the algorithms providing the possibility of separation of toroidal magnetic fields from natural spherical sources whose sizes are such that the Reynold's number for them is assessed as $10^3 - 10^5$ units. Their magnetic field obeys equation (2) [50] where diffusion, induction and hydro magnetic effects are simultaneously present. Experimental material is richly represented in reports on the two international geophysical years: 1933 and 1957/1958 as well as in published works of the worldwide magnetic survey of 1964/1965.

The above-mentioned observations were implemented on the surface of the Earth; therefore, the above-presented algorithms have been developed just for interpreting data from sparse (observational stations) and continuous (magnetic maps). A fairly full interpretation of the above observations, presented in [10], strongly supports the idea that magnetic fields observed on the Earth (the main geomagnetic field and fields of its variations) contain not only force poloidal magnetic fields but, which is more important, the toroidal non-force part. The strength of the MGF contains up to 10% of the strength of a non-force magnetic field. The strength of regular quiet solar-daily variations of the Earth's magnetic field contains up to 40% of the strength of a non-force magnetic field.

Thus, the experimental proof of the existence in a natural magnetic field of a non-force part justifies the completely above-stated theory. In this experiment with a natural magnetic field in its non-force part, the author has discovered an urgent problem of determining the true sources of the MGF and fields of its different variations. The spherical property of natural sources has been proved due to detection of a toroidal part in its magnetic field. The natural sources of the magnetic field are located in the Earth's spherical layers or on the spherical surfaces in the ionosphere.

The solution to the problem of determining the true sources of the Earth's magnetic field consists of several independent non-trivial stages.

At the first stage, it was necessary to solve the problem of interpreting both continuous and sparse data using the algorithms from the previous section. An essential usually arising difficulty is the inversion of poorly conditioned algebraic high-order matrices when determining coefficients of decomposition of a magnetic field on the sphere. This problem has been successfully solved [32] with the use of the matrices inversion of the Moor and Penrose methods adding the Tikhonov regularization [34].

The separation of fields and the calculation of the main indicator, i.e. the coefficient μ_1^1 , which is the main point of an arbitrary current system inside the sphere, is used in the calculation of the location and geometric dimensions of the electric current that causes the dipole magnetic field [32].

At the second stage, it was necessary to overcome incorrectness of the statement of the inverse problem of determining sources inside the sphere. From the classic mathematics, it is known that such an inverse problem has no solution.

In order to avoid incorrectness in the statement of an inverse problem, it is necessary to preliminarily introduce into it additional physical data about the source inside the sphere.

First, a source must be such that its magnetic field on the surface of the sphere with its force lines will repeat the magnetic field of dipole. The magnetic moment of the source inside the sphere must coincide with that of the magnetic field on its surface as well as with the magnetic moment of the annular electric current that is symmetric to the dipole field somewhere inside the sphere. The force lines of the annular current must coincide with the force lines of the observed magnetic field on the surface of the sphere and outside it.

In terms of mathematics, this looks like the following:



$$|M| = \mu_1^1 4\pi 10^{-3} R_0^3 = I\pi r_k^2, [Am^2] \quad (113)$$

where M is the magnetic moment, μ_1^1 is the coefficient of the dipole term of decomposition of the Earth's internal poloidal field [10], I is the current force in the contour with the current, r_k is the radius of the contour, R is the radius of the sphere, $4\pi 10^{-3}$ is the conversion coefficient from the dimension G_s to the dimension in A/m .

Second, the strains of the fields on the contour axis that coincides with the magnetic axis connecting the Earth's North Pole with the South Pole are assumed equal. In the first approximation, this can be expressed by the formula:

$$H_{pr}^i(0, R_0) 4\pi \cdot 10^{-3} = \frac{2\pi I r_k^2}{(R_0^2 + r_k^2)^{3/2}} \quad (114)$$

As a result, ignoring the strengths of currents in (113) and (114), we obtain:

$$2\mu_1^1 = H_{pr}^i(0, R_0) \left(1 + \frac{r_k^2}{R_0^2}\right)^{3/2}. \quad (115)$$

Expanding in a series the expression in brackets in the right-hand side of formula (115) and by restricting to the first two terms of the expansion, we obtain:

$$2\mu_1^1 = H_{pr}^i(0, R_0) \left(1 + \frac{3r_k^2}{2R_0^2}\right). \quad (116)$$

According to the calculations presented in [10], the values of the internal poloidal magnetic field on the pole as well as the coefficient of its dipole part are known:

$$H_{pr}^i(0, R_0) = 0,59473 [Gs], \quad \mu_1^1 = 0,32006 [Gs]. \quad (117)$$

In this case:

$$1 + \frac{3r_k^2}{2R_0^2} = 1,07632.$$

Whence we come to:

$$r_k = R_0 \cdot 0,22557 = 1437 \text{ km}. \quad (118)$$

Consequently, the depth to the source equals:

$$h = 4934 \text{ km}. \quad (119)$$

The calculated radius of the source with electric current accurate to 4.6% coincides with the radius of the zone F of the liquid kernel that is about 1,371 km. This value was multiply cited in geological and geophysical literature [26,27]. In addition, according to published works, the "thickness" of the layer F , is known to be, approximately, equal to 100 km.

By 1964-1965, the configuration and electrodynamic parameters of the natural source of the MGF based on the results obtained [35] are shown in figure 2. Such a natural source generates not only the known poloidal magnetic field in the Earth's atmosphere, but what is even more important, its toroidal part which is distinguished with the help of the above-presented algorithms.

Parameters of the source are the following:

The distance to the source – 4934 km;

The internal radius of the torus with current- 1437 km;

The transverse size of the torus – 3 km;

The current strength – $1,7 \cdot 10^8$ A;

The current density – $1,23 \cdot 10^{-2}$ A/m²;

The current density – $2,3 \cdot 10^{-8}$ B/m²;

The strength of the poloidal magnetic field in the source $-60Gs$

The strength of the toroidal magnetic field in the source $-3,6Gs$

The source of regular quiet solar-daily variations (S_q -variations) because of applying the algorithm [32] to the observed magnetic field was found in the second geophysical year of 1958-1959. The complete theory of interpreting S_q -variations is given in [32]. There is also given an algorithm of constructing the system of S_q -variations in the ionosphere. The spherical feature of the source is responsible for the appearance of the toroidal non-force magnetic field with S_q -variations up to 40% of its strength.

Thus, natural sources of the non-force toroidal magnetic field, being on the spherical surfaces, are in agreement with Theorem 4 [50] and, according to equation (2) [50] are the direct proof of the presence in the Earth's atmosphere of the non-force magnetic field.

The sources of the natural non-force electric field also locate in the ionosphere or in the Earth's interior. Their electric field is partitioned into two components: inductive and potential. According to formulas (24) [50], the inductive part has two components that are tangential to the Earth. According to Theorem 1, the vertical component of the inductive part is compensated by the potential part but can be reconstructed by the results of the spherical analysis of magnetic components such as S_q -variations, for example. In [10], such an analysis is done using the S_q -variations observed data. The results of this analysis are the inductive E_r^i mV/km and the potential E_r V/km components of the electric field of the external sources of S_q -variations, reconstructed on the Earth's surface (Figure 4).

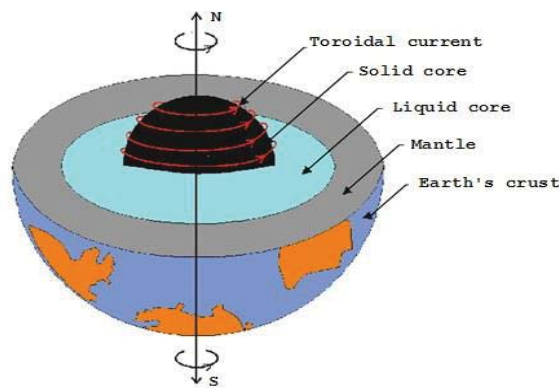


Figure 2: The source of the Earth's main geomagnetic field.

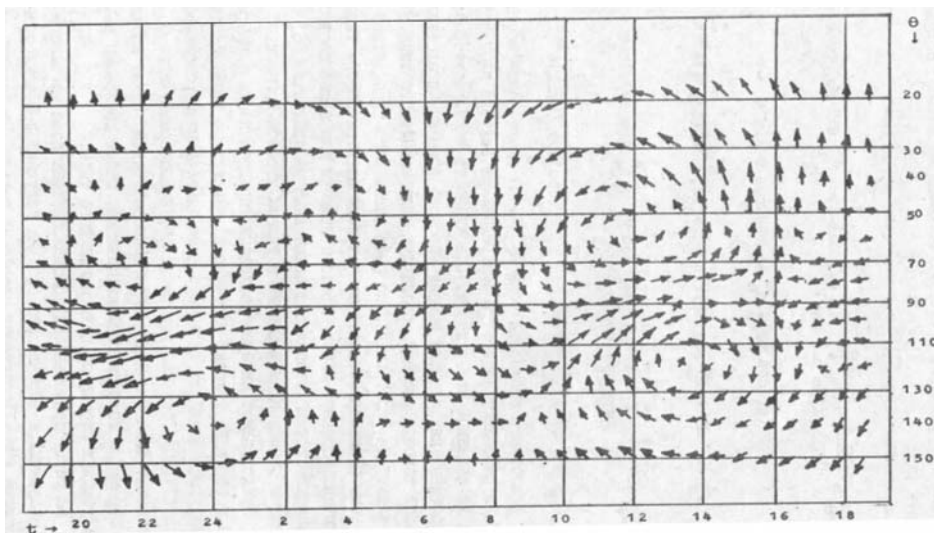


Figure 3: The source of the field of S_q variations at UT = 6 hours. Each vector corresponds to the direction and value of the surface current).

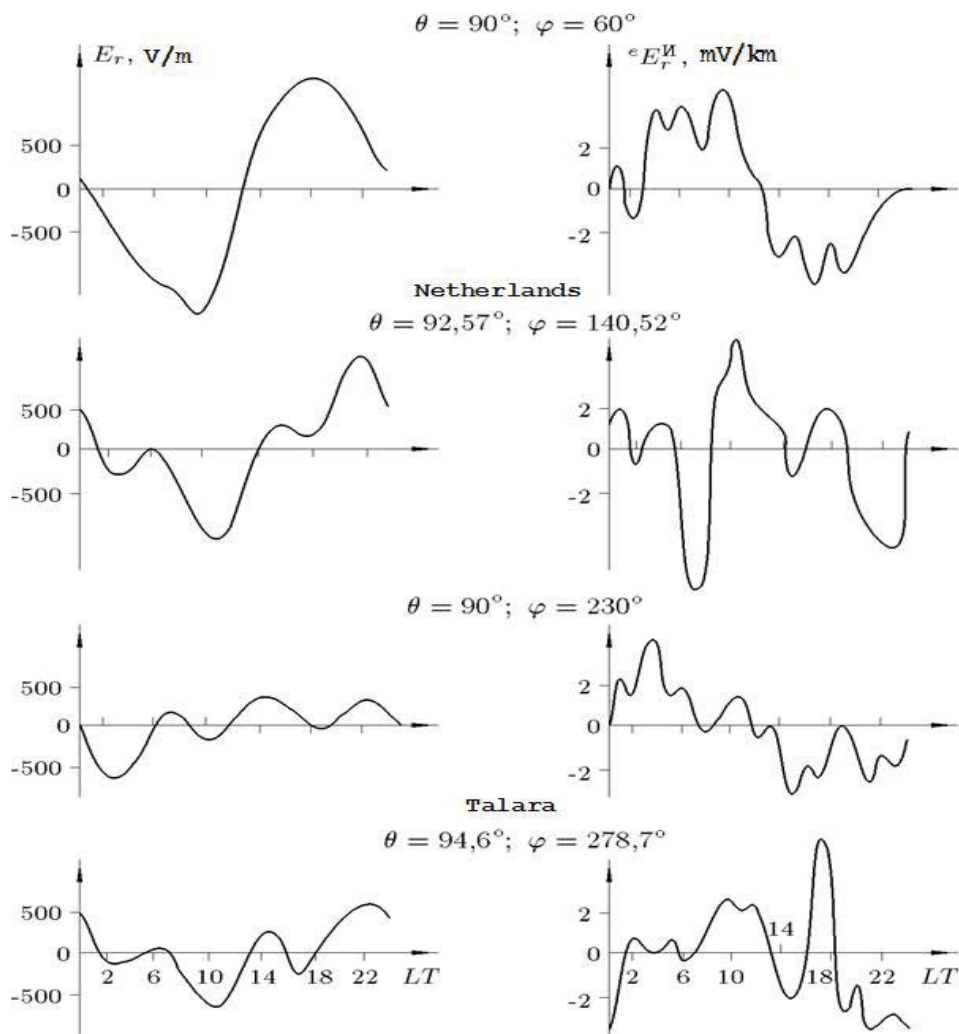


Figure 4: The electrical field at equatorial stations.

By analyzing the diagrams, one can see that the strength of the potential part is essentially higher than that in the inductive part. Therefore, the potential part screens the inductive component. The presence of the potential part can be used in applications to be described in the following section.

Manifestation of the non-force electric field in short-term earthquake precursors

The search for the earthquake precursors in well-studied physical fields continues. The results of such a search have been multiply discussed in special and scientific-popular literature. However, as for the search for precursors in physical fields, a sort of disappointment is currently observed [38]. This is not quite right, because electromagnetic and dilatant precursors, probably arising on the Earth's surface before a damaging event, have not been sufficiently studied. The possibility of appearance of precursors must be thoroughly investigated especially because one of such possibilities has been demonstrated with the help of the earlier determined system of equations of thermal electromagnetic elasticity [39,40].

In these papers, it is stated that up to the instant of the beginning of an event, the changes in the tense state of a source are expressed only in the non-force electric field, the other physical fields: the temperature field, seismic features and sound, magnetic and gravity fields arise with the presence of displacements of rocks in the source. Consequently, when the mobility of rocks in the source has already occurred its manifestation as an earthquake on the Earth's surface takes place at that very second. This fact is fixed in the thermal electro-magneto-elasticity equations. As a matter in fact, equations that are more general have not been developed yet. It is natural that the problem is to learn about a possible mobility of rocks in advance and to take measures before a damaging wave comes to the Earth's surface. The statement of this urgent problem is on demand; therefore, an adequate answer is to be found by many generations of researchers and engineers. There are, fortunately, positive examples.



Currently, there have appeared some new guesses in this area of science. Among them, there is a radical one to state that each earthquake is unique and each one occurs in its specific conditions according to a medium, where an earthquake source is generated as well as changes in stresses caused by different reasons. It looks like the triggering mechanisms of events are unique and each time different and intrinsic of only a concrete event occurred in a concrete place.

The elucidation of global reasons of the earthquakes generation is a complicated problem. In our opinion, the reasons of the earthquake formation is in the following [39]. Physical-chemical and phase processes of different intensity occur under the whole Earth’s surface at 5 km up to 700 km. This brings about weakening with a consequent violation of stiffness of the inner skeleton of the Earth’s interior, and then there appear micro-cracks, which under the action of pressure generate jointing fields that during little time concentrate into a global fault thus causing an earthquake [39].

From this standpoint, an earthquake can occur at any point of the Earth. In addition, there are areas on the Earth, where earthquakes commonly occur. Therefore, investigations are focused on studying the seismicity of earthquake-prone zones. For quite a long time seismologists are involved in the research into such zones. In addition, sources of earthquakes have been studied for a long period of time. Their models are theoretically studied with the use of computer simulation, as well as on geophysical test sites in the seismic-prone zones.

It is natural that when modeling physical processes in an earthquake source one uses common equations to describe its state. This takes place in the mathematical simulation of the behavior of such a source [39,40]. In this case, the equations contain the properties of the source medium as the Lamé parameters λ and μ . However, these parameters are so averaged, that it is impossible with their use to see the main microphysical properties of rocks of the earthquake source. In our opinion, the most important property for predicting the rocks destruction is their possible micro jointing as well as the presence of grains and pores in them. All these factors accelerate the process of jointing. Therefore, it seems that to describe the state of the earthquake focus it is more reasonable to use not the Lamé but the Rabotnov-Lomakin parameters [41]. The latter parameters set a heterogeneous medium, in which due to the presence of cracks, grains and pores, the elasticity module with tension and with compression is different. In geophysics, first this was established in [42]. The authors have analyzed the earlier obtained results of such a description of media with cracks and arrived at the conclusion about the acceptance of the description of parameters of rocks with cracks, inclusions and pores as follows:

$$\bar{\lambda} = \lambda - \nu\xi^{-1}, \quad \bar{\mu} = \mu - \nu\xi \tag{120}$$

The parameter of cracks ξ in (120) can be determined in two ways:

$$\xi = \bar{\sigma} / \bar{\sigma}_0; \quad \bar{\sigma} = \frac{1}{3}\sigma_{ii}; \quad \bar{\sigma}_0 = \left(\frac{3}{2}S_{ij} \cdot S_{ji}\right)^{1/2}; \text{ Here}$$

$$S_{ij} = \left(\sigma_{ij} - \frac{1}{3}\sigma_{kk}\delta_{ij}\right) \text{ Is the stress deviator,}$$

$$\xi = \frac{I_1}{\sqrt{I_2}}; \quad I_1 = U_{ii} \text{ Is the first invariant of the deformation tensor,}$$

$$I_2 = \left[\frac{1}{2}(U_{ij} + U_{ji})\right]^2 \text{ Is the second invariant of the deformation tensor,}$$

U_{ij} and U_{ji} are deformation tensor components, ν is the elasticity module.

In this statement, the Hook-Duhamel-Neumann deformation tensor in the cracked medium of the focus can be written down as follows:

$$\sigma_{ij} = 2\bar{\mu}U_{ij} + \delta_{ij}(\bar{\lambda}U_{kk} - \nu\sqrt{I_2} + (3\bar{\lambda} + 2\bar{\mu})\alpha(T - T_0)). \tag{121}$$

In addition, correspondingly, the system of equations for the earthquake source:

$$\rho \frac{\partial^2 \mathbf{U}}{\partial t^2} = \mathbf{e} \cdot \text{Div} \sigma_{ij} - (3\bar{\lambda} + 2\bar{\mu})\alpha \text{grad} T + [\sigma \mathbf{E} \times \mu_c \mathbf{H}] - \rho \mathbf{g} - \mathbf{F}_c,$$

$$\sigma\mu_e \frac{\partial \mathbf{H}}{\partial t} = \Delta \mathbf{H} + \sigma\mu_e (\mathbf{H} \text{grad}) \frac{\partial \mathbf{U}}{\partial t} - \sigma\mu_e \left(\frac{\partial \mathbf{U}}{\partial t} \text{grad} \right) \mathbf{H} - \sigma\mu_e \mathbf{H} \text{div} \frac{\partial \mathbf{U}}{\partial t}, \quad (122)$$

$$C_v \rho \frac{\partial T}{\partial t} = \chi \Delta T - (3\bar{\lambda} + 2\bar{\mu}) \alpha T_0 \text{div} \frac{\partial \mathbf{U}}{\partial t} + \rho Q.$$

The parameters of the earthquake source are the following:

U – The vector of displacements,

e – The unit vector directed along a maximum stress,

H – The vector of the magnetic field stress,

E – The vector of the electric field stress,

T – The temperature,

g – The vector of acceleration,

σ – The conductivity,

μ_e – The magnetic permeability of the medium in the source,

$\bar{\lambda}, \bar{\mu}$ – The Rabotnov-Lomakin coefficients,

ν – The elasticity module,

ρ – The density of the medium in the source,

σ_{ij} – The stress tensor,

$(3\bar{\lambda} + 2\bar{\mu})/3$ – The module of the manifold compression, corresponding to the cracked state of the source,

β_α – The coefficient of the volume extension,

χ – Is the thermal conductivity,

C_v – The heat capacity,

T – The initial temperature in the source,

F_c – The vector of supplementary volumetric forces (in particular, the tide forces and those arising due to the phase transformations in rocks of the source),

Q – The supplementary heat,

U_{ij} – The deformation tensor,

$I_1 = U_{ii} = \frac{\partial U_i}{\partial i}$ – The first invariant of the deformation tensor,

$I_2 = \left[\frac{1}{2} \left(\frac{\partial U_i}{\partial j} + \frac{\partial U_j}{\partial i} \right) \right]^2$ – The second invariant of the deformation tensor, δ_{ij} – The unity tensor.

The system of equations (122) describes the effects in electro-heat conductive deformable bodies (in our case these are the volumes in the earthquake –prone zone). In these volumes, the displacement currents are insignificant, the volumetric charge is also insignificant, and the joule heat releases are minor. The system is constructed based on fundamental laws of conservation and thermodynamic inequalities.

The main problem, indicated in the title of this study is the search for earthquake precursors among well studied and measurable on the site of physical fields. In this connection, the medium temperature extension (compression) forces are introduced into the balance equation under the action of supplementary heat, the Lorentz force and gravitation, as well as



“skeleton cohesive force” and the force of insertion of the rocks volume in the source. The introduction into the equation of motion of the actually skeleton cohesive force is justified, in our opinion, because we are studying the state of forces and stresses in the source before the appearance of a shift in the source resulting in generation of a shock wave causing an earthquake. The equation of balance of forces and stresses is written for the elementary volume of a source equal to 1 m^3 . The full source volume that can be sufficiently large is a part both of the left- and the right-hand sides of equations (122) therefore; it is easily normalized to unity. Physically this means that this allows the force balance to be attained with equal conditions both for the whole source and for its elementary volume (under the assumption of the fractal feature of rocks of a source). Because of this, physical processes in the elementary source volume are subject to the simulation, thus essentially simplifying the mathematical aspect of a problem.

In order to describe the temperature balance, the equation of heat conductivity is introduced into a compressible variable-module medium of an elementary source volume. The equation of induction in a compressible medium is introduced for the description of a magnetic field. In so doing, for modeling the physical fields in a variable-module source medium equations (122) being similar to equations of heat-electromagnetoelasticity are written down.

The boundary conditions on the Earth’s free daily surface for system (122) are of the conventional form:

$$\mathbf{H}_1 = \mathbf{H}_2|_S; \quad \sigma_{ij}|_S = 0; \quad \mathbf{E}_S^1 = \mathbf{E}_S^2; \quad E_n^1 = \frac{\sigma_\tau}{\sigma_0} E_n^2|_S; \quad \mathbf{U}_1 = \mathbf{U}_2|_S; \quad T_1 = T_2|_S. \quad (123)$$

Here the subscripts are as follows:

1-The air,

2-The Earth,

S - The Earth’s surface,

n - The normal to the Earth’s surface,

σ_0 - The air conductivity,

σ_τ - The Earth’s conductivity.

It is proposed to simulate the earthquake precursors in physical fields in such a way that it would be possible to answer the question: in which physical fields the short-term or intermediate earthquake precursors can exist. It is clear that the Hook-Duhamel-Neumann stress tensor as related to physical parameters of the cracked medium (121) and equation (122) written down in the Rabotnov-Lomakin phenomenological parameters cannot serve as a direct information source.

The initial data are given in the following way: the fields T, H, E at a certain time instant $t (t = 0)$ are known in the whole space and are equal to T_0, H_0, E_0 .

An earthquake occurs when the accumulated tension in one of the places of the Earth’s core exceeds the threshold value Y , after which there occurs a disruption of skeleton, inter-grain and inter-pore spaces in the source substance. There occur micro-cracks, which then concentrate into a global discontinuity. The latter causes an earthquake.

Boundary conditions (123) indicate to the fact that due to an essential difference in the conductivities σ_τ / σ_0 and the daily surface behaves as a powerful amplifier of the vertically directed electric field with the amplification factor $\sigma_\tau \gg \sigma_0$. That is why a special attention must be focused on this component of the electric field.

If one imagines that all other forces except for gravitational are absent in a source, then from the first equation of (122) follows

$$\mathbf{e} \cdot \text{Div} \sigma_{ij} - \rho \mathbf{g} = 0. \quad (124)$$

From this equation, it is easy to obtain the equation of balance for a medium with different moduli. This equation can be reduced to a standard form:

$$\rho \mathbf{g} = \bar{\mu} \Delta \mathbf{U} + (\bar{\lambda} + \bar{\mu}) \text{grad} \text{div} \mathbf{U}. \quad (125)$$

If only the inertia and the stress forces are present in a source, then from the first equation of (122) it appears possible to obtain the equation of motion in a medium with different moduli:



$$\rho \frac{\partial^2 \tilde{\mathbf{U}}}{\partial t^2} = \bar{\mu} \Delta \tilde{\mathbf{U}} + (\bar{\lambda} + \bar{\mu}) \text{grad div} \tilde{\mathbf{U}}. \tag{126}$$

If deformations are regarded to be small, then the motions considered in elasticity theory are non-intensive elastic oscillations and waves. Having applied standard transformations to (126), it becomes possible to obtain equations for longitudinal and transverse oscillations (waves) in the above-mentioned medium:

$$\frac{\partial^2 \tilde{U}_l}{\partial t^2} - c_l^2 \Delta \tilde{U}_l = 0, \quad \frac{\partial^2 \tilde{U}_t}{\partial t^2} - c_t \Delta \tilde{U}_t = 0. \tag{127}$$

Here $c_l = ((\bar{\lambda} + 2\bar{\mu}) / \rho)^{1/2}$ is the longitudinal wave velocity $c_t = (\bar{\mu} / \rho)^{1/2}$, is the velocity of the transverse wave.

The wave properties of the medium surrounding a source naturally manifest at an instant of the occurrence of a shock (fault) during an earthquake, and waves are observed on the Earth’s surface by seismological stations at sufficiently big distances from the source. Currently, many research institutions are involved in studying seismicity of seismic-prone zones. However, it has still been impossible to find a sufficiently reliable earthquake precursor. In our opinion, this is associated with the fact that seismicity near to a source or inside it manifests just at the moment of the event occurrence, i.e. with displacements in the source medium.

Foreshocks that sometimes precede an earthquake and aftershocks that take place after a strong shock are, in fact, the same events accompanied by displacements, while it is necessary to know of a tense state before an event has occurred and to what extent it is crucial and whether it can result in an earthquake. As on the Earth’s free surface the vertical stress vanishes, it is impossible to measure it. In order to elucidate in which physical fields the measured values would be directly associated with the stress tensor in a source, using equations (122) it is required to estimate these connections. To this end the reduced relations (122) and (123) [39] must be used. However, they must be written down with the phenomenological Rabotnov-Lomakin parameters in the representation of (120):

$$\begin{aligned} \frac{4\pi^2 \rho}{t^2} \mathbf{U} = & \frac{\mathbf{e}}{L} |\sigma_{ij}| - \frac{(3\bar{\lambda} + 2\bar{\mu}) \alpha T}{L} \mathbf{e} + [\sigma \mathbf{E} \times \mu_e \mathbf{H}] - \rho \mathbf{g} - \mathbf{F}_c, \quad \frac{2\pi \sigma \mu_e}{t} \mathbf{H} = \frac{\mathbf{H}}{L^2} + \frac{2\pi \sigma \mu_e |\mathbf{H}|}{Lt} \mathbf{U} - \frac{2\pi \sigma \mu_e |\mathbf{U}|}{Lt} \mathbf{H} + \frac{2\pi |\mathbf{U}|}{Lt} \mathbf{H}, \\ \frac{C_v 2\pi \rho}{t} T = & \frac{\chi}{L^2} T - \frac{2\pi(3\bar{\lambda} + 2\bar{\mu}) \alpha T_0 |\mathbf{U}|}{Lt} + \rho Q \end{aligned} \tag{128}$$

The expression for the stress tensor (121) must be added to equations (128). The reduced system of equations (128) makes possible to write down the dependences of seismic, thermal, electric and magnetic fields on the displacement moduli. From the equation of balance, we may write the equality for the displacement vector in the elastic version for a cracked medium:

$$\mathbf{U} = -\left(\frac{L^2}{\bar{\mu}} \rho \mathbf{g} + \frac{\bar{\lambda} + \bar{\mu}}{\bar{\mu}} |\mathbf{U}| \mathbf{e}\right). \tag{129}$$

From formula (129) follows that in the absence of displacements in the source $|\mathbf{U}| \neq 0$ the seismic field does not contain information about the behavior of the stress tensor, hence there are no earthquake precursors. That is why numerous seismic stations distributed all over the world are fixing the events that have already occurred at $|\mathbf{U}| \neq 0$ in the source, but they don’t give you advance notice the information about the earthquake.

From the equation of temperature, we may find the dependence of the heat field on additional heat and the displacement vector module in the non-elastic version for the cracked medium:

$$T = \frac{L^2 \rho t Q - 2\pi(3\bar{\lambda} + 2\bar{\mu}) \alpha T_0 L |\mathbf{U}|}{C_v 2\pi \rho L^2 - \chi t}. \tag{130}$$

Having analyzed expression (130) within the approximation used, we can arrive at some important conclusions. First, the temperature field is independent of stresses. Hence, in the absence of the displacements $|\mathbf{U}| = 0$ and the additional heat Q it will not differ from the initial temperature T_0 . Second, and which is most important, the temperature precursors - according to the above said are only slightly probable as the temperature field T is independent of the stresses σ_{ij} .

If the temperature field of a source is, on the average, considered constant before the motions begin, i.e. an earthquake, then from the first equation of (3) it is possible to obtain a single precursor, that is, the electromagnetic field:



$$\left[\left(\rho \frac{\partial^2 \mathbf{U}}{\partial t^2} + \rho \mathbf{g} + \mathbf{F}_c \right) - \mathbf{e} \text{Div} \sigma_{ij} \right] = \mathbf{E} \cdot \mathbf{H} \sigma \mu_e \sin \zeta. \tag{131}$$

Here ζ is the angle between the vectors of the electric and magnetic fields. According to (131), it is the electromagnetic field that must contain the information about a change in the tense state of the source that is fixed in the left-hand side of equation (131). When the rapidly increasing changes, presented by the stress $\mathbf{F}_n = \mathbf{e} \cdot \text{Div} \sigma_{ij}$ in (131) equalize and exceed the sum of the inertia, the gravity forces as well as the adhesive force of the rocks skeleton, an earthquake will occur.

The second equation from (128) for the magnetic field at $|\mathbf{U}|=0$ yields the following expression:

$$\mathbf{H} = \frac{2\pi\sigma\mu_e L |\mathbf{H}|}{(2\pi\sigma\mu_e L^2 - t)} \mathbf{U}. \tag{132}$$

In (132), the dimension of the magnetic field is given in A/m . From (132) it follows that changes in the magnetic field being at a certain level $|\mathbf{H}|$, for example, at that coinciding with the stress of the MGF directly proportionally depend on displacements. Substituting (129) to (132), we obtain:

$$\mathbf{H} = -\frac{2\pi\sigma\mu_e |\mathbf{H}|}{(2\pi\sigma\mu_e L^2 - t)} \left(\frac{L^2}{\bar{\mu}} \rho \mathbf{g} + \frac{\bar{\lambda} + \bar{\mu}}{\bar{\mu}} |\mathbf{U}| \mathbf{e} \right). \tag{133}$$

According to formula (133), we may say that in the absence of displacements, the changes in the magnetic field are at a certain constant level:

$$\mathbf{H} = -\frac{2\pi\sigma\mu_e L^3 |\mathbf{H}|}{(2\pi\sigma\mu_e L^2 - t) \bar{\mu}} \rho \mathbf{g}, \tag{134}$$

Therefore, they cannot be earthquake precursors, as they do not contain the stress tensor varying in time and in space but can appear only in initiation of displacements.

According to boundary conditions (123), the electric field component E_z that is normal to the Earth's surface and is sharply enhanced in the air at the expense of an essential difference in the Earth's conductivity σ_τ and the air conductivity σ_0 $\sigma_\tau \gg \sigma_0$. has aroused considerable interest. Having omitted intermediate expressions, let us write down the dependence E_z on the Earth's parameters and the stress tensor in the source [39]:

$$E_z = \gamma \frac{1}{\rho g_z} |\sigma_{xy}| + \delta, \tag{135}$$

Here:

$$\gamma = -\frac{\bar{\mu}(2\pi L - \frac{t}{L\sigma\mu_e})}{2\pi\sigma\mu_e L^3 |\mathbf{H}| \sin \zeta}, \quad \delta = \frac{\bar{\mu}(2\pi L - \frac{t}{L\sigma\mu_e})}{2\pi\sigma\mu_e L^2 |\mathbf{H}| \sin \zeta}.$$

Here ξ is the angle between the vectors \mathbf{E} and \mathbf{H} . The dimension of E_z in (135) is given in V/m . If the rocks in the vicinity of a source are considered to be porous and filled with a conducting fluid, what may take place with fine-focus positions of an earthquake source, then the conductivity in them can in the first approximation be assessed by the Archi law $\sigma = \alpha \sigma_1 d_0^{1-m}$, where α is a constant, σ_1 is the fluid conductivity, d_0 is the porosity, m is the consolidation index (for the rocks it is estimated as $m = 1,3;3$). In this case the coefficients γ and δ can be presented directly through the rocks porosity in the vicinity of a source. Thus, for the porous rocks we can write down:

$$\gamma \approx -\frac{\bar{\mu} t d_0^{2m}}{\alpha^2 \sigma_1^2 2\pi L^4 \mu_e^2 |\mathbf{H}| \sin \zeta}, \quad \delta \approx -\frac{\bar{\mu} t d_0^{2m}}{2\pi \alpha^2 \sigma_1^2 \mu_e^2 L^3 |\mathbf{H}| \sin \zeta}. \tag{136}$$

The dependence in (136) is power with a sufficiently high degree of the effect of porosity to be investigated based on the changes in the electric field in the vicinity of a source.

The analysis of formula (135) shows that the vertical component of the electric field explicitly and linearly depends on the stress tensor module $|\sigma_{xy}|$. Really, with the growth of the stress module this component will grow and enhance in the air by orders set by the enhancement factor σ_τ / σ_0 . Therefore the growth of E_z becomes a precursor of a future event. However from a simplified system it is impossible to find those threshold values E_z at which an "unload", that is an earthquake, occurs.



Nevertheless, studying formula (135) combined with the formula for the stresses σ_{ij} from (121) makes possible to detect this threshold having estimated the energy release at which the “unload” occurs. Moreover, by the measured electric components E_x, E_y, E_z it is possible to assess the stress tensor using its direct connection with these components. This holds out hope for a possibility to solve the problem of the assessment of stresses in the Earth by the physical electric field measured on its surface. By now, this problem has been considered unsolvable because the stress tensor tends to zero on the Earth’s surface (123). The decay of the electric field at the time of an event will make possible to evaluate admissible stresses for a certain earthquake-prone zone. The two other components of the electric field in the absence of displacements $|U|$, the supplementary heat Q , the temperature $T = 0$ and the supplementary forces F_c can be found similar to (135):

$$E_x = \gamma \frac{1}{\rho g_x} |\sigma_{xy}| + \delta, \quad E_y = \gamma \frac{1}{\rho g_y} |\sigma_{xy}| + \delta. \tag{137}$$

Here γ and δ from (135) or from (136) are used.

According to boundary conditions (123), the tangential electric components are continuous, that is why their stress in the air will not differ from their stress in the Earth from the source, which on their way suffered the influence of different noise in addition to the geometric decay. Therefore, the problem of measuring the electric fields and their selection is fairly complicated. It should be noted that according to [10], the vertical component E_z could be potential only, as its induction part is compensated by charges on the Earth’s surface. Therefore, it can be measured by a polarimetry (“hydrometric propeller”). The horizontal components E_x and E_y have both potential and inductive (tellurium) parts, the relations between them and the ways of measuring them must be investigated in the future. Nevertheless, their dependence on the stress tensor and its changes in time makes the problem of measuring the electric field on the Earth’s surface and separation in it the part dependent only on stresses in a source be challenging and promising a solution of a very important geophysical problem. The latter is associated with a short-term prediction of the beginning of an earthquake. The electric field, its vertical component, in particular, sharp changes in it, to be exact, can serve a short-term precursor, which can be noticed because of the enhancement of its daily surface of the Earth.

In order to simulate the earthquake precursors in a heterogeneous medium of a source by the search for the response in the electric field on the Earth’s surface, it is necessary to learn how to simulate stresses in a source

$$F_n = e \cdot \text{Div} \sigma_{ij}, \tag{138}$$

Depending on the module of the cracked state ξ . The behavior of the stress determines the level of electric signals at the expense of re-distribution of charges arising on edges of micro-cracks in a heterogeneous medium. Based on the definition of divergence of the tensor of the second rank we may write down:

$$F_{ni} = \sum_{j=1}^3 \frac{\partial \sigma_{ij}}{\partial x_j}. \tag{139}$$

In the Cartesian coordinate system, let us write down:

$$F_{nx} = \frac{\partial \sigma_{xx}}{\partial x} + \frac{\partial \sigma_{xy}}{\partial y} + \frac{\partial \sigma_{xz}}{\partial z}, \quad F_{ny} = \frac{\partial \sigma_{yx}}{\partial x} + \frac{\partial \sigma_{yy}}{\partial y} + \frac{\partial \sigma_{yz}}{\partial z}, \quad F_{nz} = \frac{\partial \sigma_{zx}}{\partial x} + \frac{\partial \sigma_{zy}}{\partial y} + \frac{\partial \sigma_{zz}}{\partial z}. \tag{140}$$

Now it is required to express the stress tensor components through the deformation tensor components assuming the symmetry in terms of the indices $U_{ij} = U_{ji}$. Taking into consideration the construction of the stress tensor presented in (2), after carrying out trivial transformations, obtain:

$$\begin{aligned} \sigma_{xx} &= (2\bar{\mu} - 2\xi + \bar{\lambda})U_{xx} + \bar{\lambda}(U_{yy} + U_{zz}) + (3\bar{\lambda} + 2\bar{\mu})\alpha(T - T_0), \\ \sigma_{zz} &= (2\bar{\mu} - 2\xi + \bar{\lambda})U_{zz} + \bar{\lambda}(U_{xx} + U_{yy}) + (3\bar{\lambda} + 2\bar{\mu})\alpha(T - T_0), \\ \sigma_{xz} &= (2\bar{\mu}U_{xz} - \nu U_{xx}), \quad \sigma_{xy} = (2\bar{\mu}U_{xy} - \nu U_{xx}), \quad \sigma_{yz} = (2\bar{\mu}U_{yz} - \nu U_{yy}). \end{aligned}$$

Now, substituting (141) into (140) and carrying out trivial transformations we obtain the final formulas for calculating the stress components in the elementary volume of the earthquake source and come to:



$$\begin{aligned}
 F_{nx} &= 2\bar{\mu}\left(\frac{\partial U_{xx}}{\partial x} + \alpha \frac{\partial T}{\partial x} + \frac{\partial U_{xy}}{\partial y} + \frac{\partial U_{xz}}{\partial z}\right) + \bar{\lambda}\left(\frac{\partial U_{xx}}{\partial x} + \frac{\partial U_{yy}}{\partial y} + \frac{\partial U_{zz}}{\partial z} + 3\alpha \frac{\partial T}{\partial x}\right) - \\
 &\quad - \xi\left(2\frac{\partial U_{xx}}{\partial x} + \frac{\partial U_{xx}}{\partial y} + \frac{\partial U_{xx}}{\partial z}\right), \\
 F_{ny} &= 2\bar{\mu}\left(\frac{\partial U_{xy}}{\partial x} + \frac{\partial U_{yy}}{\partial y} + \alpha \frac{\partial T}{\partial y} + \frac{\partial U_{yz}}{\partial z}\right) + \bar{\lambda}\left(\frac{\partial U_{yy}}{\partial y} + \frac{\partial U_{xx}}{\partial x} + \frac{\partial U_{zz}}{\partial z} + 3\alpha \frac{\partial T}{\partial y}\right) - \\
 &\quad - \xi\left(2\frac{\partial U_{yy}}{\partial y} + \frac{\partial U_{yy}}{\partial x} + \frac{\partial U_{yy}}{\partial z}\right), \\
 F_{nz} &= 2\bar{\mu}\left(\frac{\partial U_{xz}}{\partial x} + \frac{\partial U_{yz}}{\partial y} + \frac{\partial U_{zz}}{\partial z} + \alpha \frac{\partial T}{\partial z}\right) + \bar{\lambda}\left(\frac{\partial U_{zz}}{\partial z} + \frac{\partial U_{xx}}{\partial x} + \frac{\partial U_{yy}}{\partial y} + 3\alpha \frac{\partial T}{\partial z}\right) - \\
 &\quad - \xi\left(\frac{\partial U_{xx}}{\partial x} + \frac{\partial U_{yy}}{\partial y} + 2\frac{\partial U_{zz}}{\partial z}\right).
 \end{aligned}
 \tag{142}$$

With formulas (142), it appears possible to simulate the stress components in elementary volumes of a source by the simulation of the deformation tensor components in them. The sinus of the angle between the magnetic and the electric fields from the right-hand side of formula (131) can be found as follows. According to the known formula [14], the Lorentz force can be presented in the form:

$$\sigma\mu_e \mathbf{HE} \sin \zeta = \frac{1}{\mu_e} (\mathbf{B} \cdot \text{grad}) \mathbf{B} - \text{grad} \left(\frac{B^2}{2\mu_e} \right).
 \tag{143}$$

From formula (143), keeping in mind that $\mathbf{E} = \frac{1}{\sigma} \text{rot} \mathbf{H}$, we find:

$$\sin \zeta = \frac{\frac{1}{\mu_e} (\mathbf{B} \cdot \text{grad}) \mathbf{B} - \text{grad} \left(\frac{B^2}{2\mu_e} \right)}{\mu_e \mathbf{H} \text{rot} \mathbf{H}}.
 \tag{144}$$

Now, formula (144) can be transformed by changing the differential operators by their analogs using the size of the focus L and selecting the vertical direction for the magnetic field:

$$\sin \zeta = \frac{|\mathbf{B}| \mathbf{H} \frac{1}{L} - \frac{1}{2L} (\mathbf{H} \cdot \mathbf{B})}{\mu_e \mathbf{H} \frac{1}{L} \mathbf{H}} = \frac{|\mathbf{H}|}{H_z} - 0,5.
 \tag{145}$$

Formula (145) allows the use in the simulation of any initial levels of the magnetic field $|\mathbf{H}|$ and any of its current states calculated by formulas (133) or (134). Thus, the following formula is subject to the numerical simulation:

$$\mathbf{E} = \mathbf{F}_n / (\sigma\mu_e \mathbf{H} \sin \zeta) = \mathbf{F}_n / (\sigma\bar{\mu} \mathbf{H} (|\mathbf{H}| / H_z - 0,5)).
 \tag{146}$$

The dimension of the electric field in (146) is given in V/m . In this case, a precursor must be found in the vertical component of the electric field $E_z^1 = E_z^2 \sigma_\tau / \sigma_0$. In the latter formula, E_z^2 is given by expression (146), in which the geometric decay arising due to the replacement of the field E_z^2 from the depth of the source towards the Earth's surface:

$$E_z^1 = E_z^2 \frac{\sigma_\tau}{\sigma_0 h^3} = \frac{\sigma_\tau \mathbf{F}_{nz}}{\sigma_0 \sigma \mu_e H_z (|\mathbf{H}| / H_z - 0,5) h^3}.
 \tag{147}$$

Here h - is the value reflecting the relation of the source depth H and the linear size of the elementary volume in the source $l=1m$, then $h = H/l$ In formula (147) it is better to set the strength of the magnetic field H_z at the level of the strength of the Earth's MGF because this field is surely present in a source independent of the tense state in it. The arising electric field must be controlled by the difference:

$$\left| \left(\rho \frac{\partial^2 U_\zeta}{\partial t^2} + \rho g_\zeta + F_C \right) - F_{nz} \right| \leq 0.
 \tag{148}$$



The electric field must be “interrupted” by the difference in (148), which must tend to zero at the time instant of an earthquake. This is because when an earthquake takes place, there occurs an immediate drop in stresses up to a certain level at which a new balance of forces and stresses in the source arises. This drop is usually repeated several times and is accompanied by shocks causing the displacements U at the expense of which the electric field is subject to other laws and equations and can suffer an essential drop.

The electric field cannot be simulated using formula (147) without developing the way of modeling the new parameters $\bar{\lambda}$ and $\bar{\mu}$. These parameters contain the elasticity module ν which is better to assign in a wide range of values for studying the behavior of the stress F_n and in its connection the electric field E_z^1 . In addition, $\bar{\lambda}$ and $\bar{\mu}$ contain the cracks parameter ξ which must also be simulated, for example, $\xi = I_1 / \sqrt{I_2}$. As is known, the first invariant of the deformation tensor I_1 coincides with the diagonal element of the deformation tensor $I_1 = U_{ii}$. Therefore with the multifold compression of the elementary volume $U_{ii} = P/K$, where P is the pressure per unity of the elementary medium volume K is the shift compression module and $\sqrt{I_2} = U_{ij}$ in the isotropic medium. The complicated effect on the elementary medium volume can be decomposed to the manifold compression and shift:

$$U_{ij} = \frac{1}{9K} \delta_{ij} \sigma_{ii} + \frac{1}{2\mu} (\sigma_{ij} - 1/3 \delta_{ij} \sigma_{ii}). \tag{149}$$

Bearing in mind the fact that the elementary source volume in question, the value σ_{ij} under the action of all-sided pressure can be expressed as $\sigma_{ij} = -P\delta_{ij}$, and $\delta_{ij} = 3$. In these assumptions, the required relation will have the form:

$$U_{ii} / U_{ij} = \frac{2\mu(3\lambda + 2\mu)}{9\lambda^2 + 12\lambda\mu + 4\mu^2}. \tag{150}$$

In formula (150), a known relation between the shift compression module and the Lamé parameters $K = (\lambda + 2 / 3 \mu)$ is used.

Thus, for the simulation of the parameters $\bar{\lambda}$ and $\bar{\mu}$ in the first approximation, we can use the following formulas:

$$\bar{\lambda} = \lambda - \nu \frac{9\lambda^2 + 12\lambda\mu + 4\mu^2}{2\mu(3\lambda + 2\mu)}, \quad \bar{\mu} = \mu - \nu \frac{2\mu(3\lambda + 2\mu)}{9\lambda^2 + 12\lambda\mu + 4\mu^2}. \tag{151}$$

According to (151) the new parameters non-trivially depend on the classical Lamé parameters λ and μ .

In order to find the values of the electric field in a different-scale module of a source, it is required to simulate the stress components in the source: F_{nx}, F_{ny}, F_{nz} . To this end, formulas (142), in which it is required to assign in some way the deformation tensor components, are the following:

$$U_{xx} \approx ax^2, \quad U_{yy} \approx by^2, \quad U_{zz} \approx cz^2, \quad U_{xy} \approx dxy^2, \quad U_{xz} \approx ezt^2, \quad U_{yz} \approx fzt^2. \tag{152}$$

In this case, we assume the following:

$$d \approx 0,5a; \quad e \approx 0,5b; \quad f \approx 0,5c. \tag{153}$$

In doing so, the coefficients a,b,c are not set. They can be found after the expert estimation of potential forces F_{nx}, F_{ny}, F_{nz} of stress accumulation. If $T = cont.$, all necessary derivatives are predetermined.

Then we write down the stress components using formulas (142):

$$F_{nx} = (3\bar{\mu} + \bar{\lambda} - 2\nu)at^2 + \bar{\mu}bt^2, \quad F_{ny} = -vat^2 + (2\bar{\mu} + \bar{\lambda} - \nu)bt^2 + \bar{\mu}ct^2. \tag{154}$$

In order to calculate the unknown coefficients a,b,c it is needed to imagine the initial state of an earthquake source with the parameters $F_n, \nu, t, \lambda, \mu$ to expertly assign them and after that to define unknown coefficients a,b,c and with their help – the coefficients d,e,f .

When selecting a medium model and the source geometry for the calculation, it is best of all to make use of a well-known in literature example. The Earth’s upper mantle parameters in this example are the following:

$$\lambda = 50 \times 10^9 Pa, \mu = 30 \times 10^9, \quad \nu = 10^9, \quad |F_n| = 10^6 Pa, |H| = 39,8 A / m \sigma_\tau / \sigma_0 = 10^3,$$

$$h = 2 \times 10^4, \quad g_z = 9,8 m / c^2, \rho = 2800, kl / m^3,$$



The parameters in the source are $H = 20 \text{ km}, \sigma = 0,1 \text{ Sm} / \text{ m } \rho = 4800 \text{ kl} / \text{ m}^3$

The initial parameters of the holding medium presented here made possible to calculate the coefficients a, b, c, d, e, f that are required for the simulation of the stresses F_n in terms of the cracks module ξ . Table 1 presents their values.

For detecting the stress changes in the source and changes in the electric field on the Earth's surface in terms of the cracks module ξ in the source, the calculations of these values are presented in table 2.

The analysis of table 2 shows that stresses essentially depend on the cracks module of a different scale medium although the Rabotnov-Lomakin parameters do not strongly respond to the behavior of this module. At a certain time instant, the stresses change their signs thus indicating to a considerable influence of different moduli. With a "strong" difference in moduli, the all-sided pressure can change a sign resulting in a shift. This predetermines the appearance of a shock because of a possible shift. In this case, the electric field on the Earth's surface E_z^1 also changes its sign and this can be an essential characteristic feature in the behavior of the electric field in terms of the cracks development. In this case, the values of the electric field are measurable. Although one should, bear in mind that the problem of selecting a signal from an earthquake against other numerous sources of a potential electric field in the atmosphere is not even set here. For setting this problem, it is necessary to carry out not only theoretical but also field surveys as well. The diagrams of the electric field observed in situ several hours before an earthquake begins are presented in [10]. The measurements presented were made by Turkish researchers [43] and are the first field experiments as associated with the ideas and estimations of the electric field above the source of a real earthquake.

The simulation of the behavior of stresses in an earthquake source indicates to the fact that changes in the tense state of a source can be fix data distance from the Earth's surface by measuring and tracing the behavior of a non-force potential electric field. This field if thoroughly investigated may act as a precursor of a potential earthquake. All other physical fields measurable on the Earth, i.e. seismic, thermal, magnetic, gravitational do not contain earthquake precursors because they respond only to an event that has already occurred.

The non-force magnetic field in the Aharonov-Bohm experiment

In addition to natural phenomena in one way or other containing toroidal non-force electromagnetic fields, these fields arise in laboratory experiments. The most significant among them is the above-mentioned Aharonov-Bohm effect [44]. In this experiment, a quantum particle when flying across an infinitely long solenoid with electric current suffers the deviation in the trajectory in spite of the fact that outside such a solenoid the magnetic field in its classical definition equals zero $H = \nabla \times A = 0$ (Figure 5) [44].

It is considered that the interaction of particles proceeds with a vector potential because of $A = \nabla\phi$ although the scalar potential ϕ is not a physical object. According to the electrodynamics proposed, a quantum in the Aharonov-Bohm effect suffers the interaction not with the scalar potential ϕ , i.e. a mathematical function, but with a non-force toroidal magnetic field. That is why we are interested in the following: whether a certain physical object remains in space outside the source if $\nabla \times A = 0$, and whether the Stokes theorem about the circulation of the vector A over a closed contour if $\nabla \times A = 0$ is still valid. In [45], there is a negative answer. In our opinion, the Stokes theorem is also valid in this case. Moreover, a physical object, i.e. a toroidal non-force magnetic field, determined with the help of (6) is still in space outside the source. Really,

Table 1:

$$F_{nx} = F_{ny} = F_{nz} = E_z^1 = 10^6; \nu = 10^9; \lambda = 50 \times 10^9; \mu = 30 \times 10^9; t = 10$$

<i>a</i>	<i>b</i>	<i>c</i>	<i>d</i>	<i>e</i>	<i>f</i>
5,85×10 ⁻⁸	6,81×10 ⁻⁸	9,60×10 ⁻⁸	2,93×10 ⁻⁸	3,40×10 ⁻⁸	4,8010 ⁻⁸

Table 2:

$\xi \times 10^9$	$\bar{\lambda} \times 10^{10}$	$\bar{\mu} \times 10^{10}$	F_{nx}	F_{ny}	F_{nz}	E_z^1
1	4,97	2,97	1,00×10 ⁶	1,02×10 ⁶	1,02×10 ⁶	167,59
10	4,71	2,71	8,22×10 ⁵	8,27×10 ⁵	7,37×10 ⁵	120,62
20	4,43	2,43	6,21×10 ⁵	6,18×10 ⁵	4,19×10 ⁵	68,50
30	4,14	2,14	4,21×10 ⁵	4,08×10 ⁵	1,00×10 ⁵	16,39
40	3,86	1,86	2,20×10 ⁵	1,99×10 ⁵	-2,18×10 ⁵	-35,70
50	3,57	1,57	1,87×10 ⁵	-1,10×10 ⁴	-5,37×10 ⁵	-87,84
60	3,29	1,29	-1,82×10 ⁵	-2,21×10 ⁵	-8,56×10 ⁵	-139,96
70	3,00	1,00	-3,83×10 ⁵	-4,30×10 ⁵	-11,7×10 ⁵	-192,07
80	2,71	0,71	-5,84×10 ⁵	-6,40×10 ⁵	-14,9×10 ⁵	-244,19

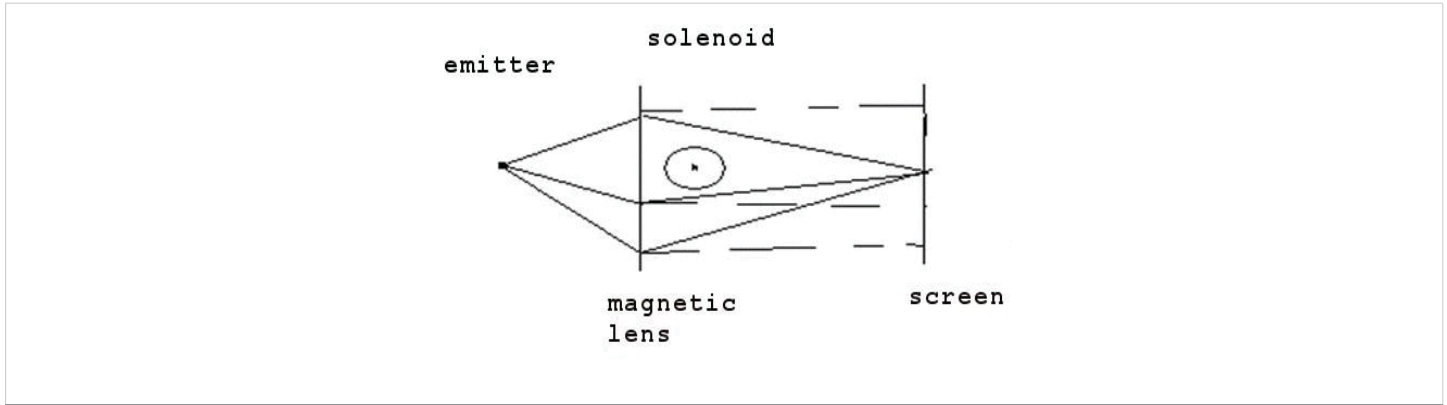


Figure 5: The Aharonov-Bohm effect.

$$\oint (\mathbf{A} \cdot d\mathbf{l}) = \oint (\nabla \times \mathbf{A} \cdot d\mathbf{s}) = \oint (\mathbf{H}_T \cdot d\mathbf{s}) + \oint (\mathbf{H}_p \cdot d\mathbf{s}) \tag{155}$$

Let now $\nabla \times \mathbf{A} = 0$ then $\nabla \times [(\mathbf{Q}\mathbf{r}) + \nabla \times (\mathbf{Q}\mathbf{r})] = 0$. Hence $\nabla \varphi = [(\mathbf{Q}\mathbf{r}) + \nabla \times (\mathbf{Q}\mathbf{r})]$.

This is the same as:

$$\mathbf{H}_T = \nabla \varphi - (\mathbf{Q}\mathbf{r}) \tag{156}$$

Here φ and Q are different from zero arbitrary scalar functions of the class C^∞ .

Now let the poloidal magnetic field outside the source be equal to zero ($H_p = 0$). In this case, with allowance for (156), we have:

$$\oint (\mathbf{A} \cdot d\mathbf{l}) = \oint (\nabla \times \mathbf{A} \cdot d\mathbf{s}) = \oint (\mathbf{H}_T \cdot d\mathbf{s}) + \oint (\nabla \varphi - (\mathbf{Q}\mathbf{r})) \neq 0 \tag{157}$$

From (157) it follows that there may be a situation when in spite of the fact that $H_p = 0$, the toroidal non-force field H_T may not be equal to zero because of the initially different from zero scalar potentials φ and Q or their difference which in (157) differs from zero. In this case, the Stokes theorem due to (157) and contrary to the analysis given in [45] is valid.

Indeed, let in the space \mathbb{R}^3 along the coordinate z of a rectangular coordinate system x,y,z there be an infinitely long solenoid with a dense winding, at the center of the cylinder of which there is also a fixed spherical coordinate system, in addition to a rectangular one. In the solenoid, there circulates a constant electric current with the density J or an alternating current with the density $J e^{i\omega t}$. According to standard Maxwell's equations, these currents are related to the vector potential by the equations $\nabla \nabla \cdot \mathbf{A} - \nabla \times \nabla \times \mathbf{A} = \mathbf{J}$ or $\nabla \nabla \cdot \mathbf{A} - \nabla \times \nabla \times \mathbf{A} + \chi^2 \mathbf{A} = \mathbf{J}$, where $\chi = (i\omega\mu\sigma)^{1/2}$. The multiplier $e^{i\omega t}$ in the latter is omitted. It is clear that only the ϕ -component of the current density J_ϕ circulates in the solenoid. Let us map the first equation onto the ϕ -axis of the spherical coordinate system:

$$-j_\phi = \frac{1}{r \sin \theta} \frac{\partial}{\partial \theta} \sin \theta \frac{\partial A_\phi}{\partial \phi} + \frac{1}{r^2 \sin \theta} \frac{\partial^2 A_\phi}{\partial \phi^2} + \frac{1}{r} \frac{\partial^2 r A_\phi}{\partial r^2} + \frac{\cos \theta}{r^2 \sin^2 \theta} \frac{\partial A_\theta}{\partial \phi} - \frac{\cos \theta}{r^2 \sin \theta} \frac{\partial A_\phi}{\partial \phi} + \frac{1}{r^2} \frac{\partial}{\partial \theta} \frac{1}{\sin \theta} \frac{\partial}{\partial \theta} \sin \theta A_\phi - \frac{1}{r} \frac{\partial^2 A_\phi}{\partial \theta \partial \phi} + \frac{2}{r^2 \sin \theta} \frac{\partial A_r}{\partial \phi} \tag{158}$$

If we map the second equation, then one more term will be added to (158) $\chi^2 A_\phi$. It is easy to notice that, according to definition (6) [50], the latter term in (158) is the doubled intensity of the $H_{T\theta}$ -component of the non-force magnetic field H_T , $\frac{2\partial A_r}{r^2 \sin \theta \partial \phi} = \frac{2}{r \sin \theta} \frac{\partial Q}{\partial \phi} = \frac{2}{r} H_{T\theta}$ just divided by the coordinate r . Therefore, expression (158) is a direct proof of the generating by the current of the conductivity (J_ϕ -component) of a non-force component of the magnetic field H_T , which, according to formula (157), remains in space even with \mathbb{R}^3 . This circumstance ensures the interaction of a quantum particle with a non-force toroidal magnetic field, but not with a vector potential.



The Aharonov-Bohm quantum effect is caused by the same magnetic field, but by its non-force part. Moreover, the Stokes theorem holds in this case as well. The dualism of the vector potential A in its non-standard definition (5) is confirmed by the Aharonov-Bohm effect.

On the mutual generation of non-force and force magnetic fields in tokamak and its suppression

The review [46] is dealt with the history of developments and experimental verification of the idea of implementing a controlled thermonuclear reaction in tokamaks. As follows from the review, numerous experiments in tokamaks have not yet led to the expected result. The main reason for this failure is the unstable plasma behavior in the tokamak “donut”. The causes of the instability have been studied in detail [46].

In our opinion, the main cause of plasma instability (it is secondary) in a tokamak “donut” is the mutual generation of a toroidal two-component magnetic field of 5 T strength and higher, created inside a tokamak, with a poloidal field of conductors located on the outer side of the tokamak, exciting a poloidal field with “Preload” of the heated plasma to the center of the toroidal cavity of the tokamak and “release” of the plasma from the walls of the tokamak. In this basic construction, as it seems, one important circumstance, described in detail in [9,12], is not taken into account. This circumstance is due, as is mentioned above, to a possible self-generation of the main toroidal magnetic field H_T inside the tokamak “donut” with a poloidal field H_p .

In fact, if we define H_T and H_p , as is proposed above, with the help of a chain of the equalities:

$$\nabla \cdot \mathbf{H} = 0, \quad \mathbf{H} = \nabla \times \mathbf{A}, \quad \mathbf{A} = (Q\mathbf{r}) + \nabla \times (Q\mathbf{r}), \quad \mathbf{H}_T = \nabla \times (Q\mathbf{r}), \quad \mathbf{H}_p = \nabla \times \nabla \times (Q\mathbf{r}). \quad (159)$$

Then from (159) follows relation (10) in [50]

$$\nabla \times \mathbf{H}_T = \mathbf{H}_p, \quad \nabla \times \mathbf{H}_p = \chi \mathbf{H}_T, \quad (160)$$

Where H_T is the toroidal magnetic field, originally created in the tokamak “donut”, H_p is the poloidal normal field of the external conductors H_T . Here $\chi = \frac{\gamma}{\eta}$, γ is the diffusion rate of the magnetic field, $\eta = \frac{1}{\mu\sigma}$ is the magnetic viscosity.

The non-stationarity in a tokamak arises at the moment when the electric field is turned-on to initiating a movement of the produced plasma along the tokamak “donut”. At this instant, a self-excitation and an uncontrolled increase in the magnetic field of various topologies (other than toroidal) occur at the expense of the magnetic field itself inside the tokamak if there is a conducting plasma inside the tokamak and sufficient plasma conductivity ($\chi \neq 0$). This brings about the appearance of an uncontrolled (secondary) instability of the plasma pinch.

The estimation of self-excitation in the large MTP model from [46], according to definitions (159), (160), is as follows. If we accept that $\nabla \times \approx \frac{1}{L}$, where L is the linear size of the plasma cord inside the tokamak, then we have

$$\frac{1}{L} \mathbf{H}_p \approx \frac{\gamma}{\eta} \mathbf{H}_T, \quad \frac{1}{L} \mathbf{H}_T \approx \mathbf{H}_p. \quad (161)$$

Let a small radius of the plasma cord be equal to $R = 2m$, then $L = 2\pi R = 4\pi m$, and the intensity of the toroidal field $|\mathbf{H}_T| \approx 5 T$. Then the intensity, excited by the toroidal magnetic field, of the additional poloidal magnetic field will be of the order:

$$|\mathbf{H}'_p| = \frac{5}{4\pi} \approx 0,4 T. \quad (162)$$

The estimation of the diffusion rate over the primary fields will be:

$$\gamma = \frac{\eta}{L} \frac{|\mathbf{H}_p|}{|\mathbf{H}_T|}. \quad (163)$$

An additional toroidal magnetic field will grow by the value:

$$\mathbf{H}'_T = \frac{\eta}{\gamma L} \mathbf{H}'_p. \quad (164)$$

The process of self-excitation will increase due to the mutual generation of magnetic fields, as a result of which the very “breakdown” occurs. At the same time, as the temperature inside the tokamak increases, the diffusion rate will also increase (163) due to a drop in conductivity in the plasma string and an increase in the poloidal field inside the tokamak.



Currently, the electrodynamics in tokamak is described by the well-known classical Maxwell's equations, which somewhat differ in their essence from equations (160).

The above-said suggests an idea of solving the problem of suppressing self-generation by uninterrupted exclusion of a strong poloidal magnetic field inside the tokamak by means of the outer poloidal magnetic field directing in the anti-phase to arising in the tokamak "donut" magnetic field [12].

In existing tokamaks, a poloidal (transverse to toroidal) magnetic field is initially generated [46]. An external poloidal magnetic field is necessary also because of suppressing a strong poloidal magnetic field arising due to self-generation. In a tokamak, when the plasma is confined, it is necessary to preserve the original toroidal magnetic field and a weak poloidal one. When confining plasma, it is necessary not to generate a strong transverse (a poloidal magnetic field), but to reduce the transverse field by any means in order not to contribute to the self-generation of these magnetic fields [9,12]. This greatly reduces the penetration of particles to the tokamak walls. Plasma particles will "wind up" only on the "force" lines of the toroidal magnetic field parallel to the walls. Similar physical phenomena occur in the mirror cells.

Non-force variable electromagnetic fields of displacement currents in capacitors

The bias currents introduced into the equations of the electromagnetic field in the nineteenth century by Maxwell are clearly realized in electric capacitors. Their indispensable presence in the capacitors of oscillating circuits (induction coil - capacitor) interests physicists not only from the point of view of the implementation of capacitors in various technical devices, but also from the point of view of the emerging electromagnetic fields in capacitors with alternating electric current [47].

Probably, the most interesting problem for many researchers is whether the bias current in capacitors has a magnetic field, and if so, what is its nature. The answer to this question is not known with certainty. There are two opposing points of view: one of them denies the existence of a magnetic field, the other one relies on the experimentally recorded magnetic field [47]. If we agree with the experiment conducted in [47], then we can consider that the problem of the existence of a magnetic field of bias currents in capacitors has been solved. However, skeptics present a simple argument against the experiment, referring to the fact that capacitors, in contrast to inductors, are not customarily shielded from the bias magnetic field. In addition, this is true.

It turned out that the whole thing is in the nature of those electromagnetic fields, which, apparently, nevertheless exist and are caused by the bias currents.

In order to elucidate the nature of the electromagnetic fields of bias currents in capacitors, it is necessary to investigate the nature of the electromagnetic fields of bias currents, possibly, existing not only in capacitors.

In this connection, the literature on physics, as well as everything stated in the previous sections, indicate to the fact that in nature there can exist both force electromagnetic fields according to Lorentz's interpretation and non-force electromagnetic fields, the equations for which somewhat differ from the standard Maxwell's equations [36].

The basic properties of non-electromagnetic fields are explained in the previous sections. The existence of these properties is important for understanding the nature of the electromagnetic field of the bias currents both as they are and the bias currents in capacitors, in particular. This understanding reduces to the two simple facts. The vortices of a non-force magnetic field H_T do not excite an electric current, but pass on to a force poloidal magnetic field at the expense of $\nabla \times H_T = H_p$. A non-force poloidal electric field due to $\nabla \times E_p = 0$ does not possess an E. D. S. induction. Its presence in capacitors is caused by varying electric charges on capacitor plates as well. It has the potential, by definition.

In order to present an example and understand what kind of strengths the non-force electromagnetic fields have, let us consider an example of a capacitor,

Which was experimentally studied in [1]. The bias current density, according to [3], (formula 20) has the form:

$$\mathbf{j}_{\vec{n}} = \frac{\partial \mathbf{D}_p}{\partial t} = \chi \mathbf{H}_T = -(\mu \omega^2 \varepsilon)^{1/2} \mathbf{H}_T. \quad (165)$$

On the other hand, in a capacitor, according to [47], the bias current is:

$$\mathbf{j}_{\vec{n}} = -\varepsilon \frac{U_0}{d} \omega \sin \omega t. \quad (166)$$

Here U_0 - is the strength on the capacitor plates, directed from one plate to another, d - is the distance between the plates. From (165) and (166), we can obtain



$$(\varepsilon\omega^2\mu)^{1/2}\mathbf{H}_T = \varepsilon\frac{U_0}{d}\omega\sin\omega t \quad (167)$$

Thus, we obtain the value of the toroidal non-force magnetic field in Oersted:

$$|\mathbf{H}_T| = \sqrt{\frac{\varepsilon}{\mu}}\frac{|U_0|}{d}4\pi10^{-3}|\sin\omega t| \quad (168)$$

In the air capacitor, the magnetic field will have the following form:

$$|\mathbf{H}_T| = \sqrt{\frac{\varepsilon_0}{\mu_0}}\frac{|U_0|}{d}4\pi10^{-3}|\sin\omega t| \quad (169)$$

Then the capacitor parameters are taken from [47]. Now:

$$\sqrt{\frac{\varepsilon_0}{\mu_0}} = 2,7 \cdot 10^{-3}, \quad |U_0| = 20 [V], \quad d = 5 \cdot 10^{-2} [i], \quad |\sin\omega t| \approx 1 \quad (170)$$

In these parameters, the non-force magnetic field will be equal to:

$$[\delta] = [orsted] \quad (171)$$

Such an insignificant magnetic field in the capacitor [47] is, as it is, not dangerous because of its non-force nature. According to formula (2) [50] it does not generate electric current in the environment and in devices surrounding the capacitor. Therefore, capacitors generally do not screen from the magnetic field. The electric field of the capacitor $|\mathbf{E}_p| = \frac{|U_0|}{d} \approx 400 [V/m]$ is also not dangerous because it does not generate EMF in the environment and devices surrounding it. The user must not touch a functioning capacitor because of the strength in it.

Hence there is a possibility to make use of contrary opinions of physicists and engineers. The magnetic field in capacitors is generated by displacement currents, but it is non-force and of low strength, and does not excite the electric current in the surrounding space. The electric field of the capacitor does not also generate the induction of EMF in spite of the variable in time nature. This is the field of charges varying on the capacitor plates, which provides a continuous course of the electric current in the circuit containing a capacitor. A magnetic needle does not respond to a rapidly changing strength of the non-force magnetic field due to the intrinsic of it sluggishness.

In the nature, a non-force magnetic field is fixed by the world network of magnetic stations with magnetometers measuring the constant magnetic field and its slow variations with respect to time. The needle devices and those similar to them including proton ones manage to fix these slow changes of the total, i.e. force and non-force, magnetic field. A detailed analysis of the non-force natural electromagnetic fields can be found in [10].

Non-force variable magnetic fields and skin-effect

Solving the problem of increasing the depth of surveying the Earth's interior with the use of a variable electromagnetic field is one of the most important problems in geophysical prospecting.

However, the depth of studying the Earth's crust using the variable electromagnetic field is restricted by the influence of the skin effect that arises with increasing the electromagnetic field frequency.

The skin-effect and its influence on the electric field and currents are considered in detail in [14] and are expressed in that the electromagnetic field of the secondary electric current is induced in a medium in the counter-phase to the primary field; hence, it compensates the primary electromagnetic field, enabling its penetration into a conductor at a considerable depth. Therefore, high-frequency methods of electric prospecting having a high resolvability are applied only in the low-depth geophysics. This, for example, is in the methods using georadars.

For overcoming this essential difficulty, as it seems, in geophysical prospecting one can employ non-force variable electromagnetic fields whose properties as related to the skin effect are essentially different from the known force electromagnetic field fixed in Maxwell's equations.

In published works, one can often come across the information about the creation of laboratory sources of a non-force



electromagnetic field. In this connection, we can recall Bullard's efforts of creating such a source with the help of one-disk construction [48]. Rikitaki [49] attempted in creating a source of a non-force electromagnetic field based on a two-disk construction. The fact is theoretical experiments have not yet been technically implemented.

The author has detected natural sources of a non-force electromagnetic field. It has been proved that electric currents on the spherical surfaces, for example, in the ionosphere, or in the Earth's spherical layers along with a force electromagnetic field simultaneously generate a non-force part of the electromagnetic field. Interpreting the world data on the electromagnetic field in international geophysical year (1933, 1957/1958) with the algorithms based on (36), it appeared possible to verify on experimental data the presence of a non-force electromagnetic field in natural sources [10]. A positive result of the verification has enabled the author to indicate to the necessity of taking into account a non-force part of the electromagnetic field when interpreting data in conventional methods of geophysical prospecting (magneto-telluric sounding and time-domain measurements on major periods).

In such data, a non-force electromagnetic field is obligatorily present due to the spreading of sources over the spherical ionosphere and the Earth because of the Earth's spherical effect. The influence of spherical properties of sources manifests in the appearance of a non-force part of the electromagnetic field, which, if not taken into account, acts as an unresolvable error in interpretation of measurements data.

Nevertheless, detecting natural sources stimulates the creation of artificial sources of a non-force electromagnetic field for the prospecting purposes. Such a possibility, in our opinion, is substantiated by one of equations (36). The following equation:

$$\frac{\partial \mathbf{D}_P(\cdot)}{\partial t} = -\chi \mathbf{H}_T'(\cdot) \quad (172)$$

Makes it apparent that the creation of such an artificial source by the way, for example, of the excitation by a capacitor with a strongly polarizing material between the plates of a rapidly varying in time electric induction of a poloidal field is quite possible. According to (172), these changes bring about the appearance of a toroidal non-force magnetic field H_T , whose spreading into the environment will give an expected effect of arising a controlled spreading of a non-force electromagnetic field.

The main thing is that according to (36), the non-force magnetic field does not excite electric currents in the surrounding space. This removes the skin-effect. Therefore, there is a probability that a non-force electromagnetic field may penetrate into a surrounding conducting medium at a much greater depth than a force magnetic field [10].

The skin-effect essentially restricts the penetration of a variable electromagnetic field into a conducting magnetic medium according to the following formula [14]:

$$\delta^n = \left(\frac{2}{\omega \mu \sigma} \right)^{1/2}, \quad (173)$$

where δ^c is the depth of penetration of the force field, ω is the circular frequency of the excited magnetic field, μ is the magnetic penetrability σ is the conductivity of the medium of the electromagnetic field penetration up to the point, where the electric field vector is equal to $1/e$ of the value on the surface ($e = 2,7182$).

Let an amplitude of the force electromagnetic field A^c on the surface of a conductor be equal to that of the non-force electromagnetic field A^{nc} .

During the propagation of the magnetic field, its decrease is also subject to the geometric law. For a force field, the amplitude decreases as follows $A^c / (h^3 e)$, h is the depth of the geometric attenuation. For a non-force field, due to the absence of a skin-effect, the amplitude decreases by A^{nc}/h^3 . Then the ratio of penetration depths of the non-force electromagnetic field to the force one will be:

$$\delta^{nc} / \delta^c = e. \quad (174)$$

When a magnetic field is spreading, its decrease obeys the geometric law as well.

This rather a rough estimation means that penetration of a non-force electromagnetic field into a medium would be almost a factor of 3 deeper, thus essentially extending the potentialities of the prospecting of the Earth's interior by means of a non-force electromagnetic field at high frequencies.

We should once again mention that a slowly changing non-force electromagnetic field must be measured as follows: a magnetic field by a magnetometer, an electric field – by an electrometer as is fixed in equations (36).



Thus, an arising prospect of increasing the depth of geophysical surveys with the use of a non-force electromagnetic field must stimulate the interest towards the creation of devices being able to provide exploitation of a non-force electromagnetic field in geophysical practice, geophysical prospecting included.

Superdeep sounding of the Earth with a non-force magnetic field

The superdeep sounding of the Earth with the use of a magnetic field of quiet solar-daily variations have been repeatedly carried out. However, there were discovered essential differences in depths up to a conducting layer, which were experimentally determined at various points of the Earth, while temporal frequencies were not distinguished. Moreover, in the magnetic field of S_q -variations there were fixed effects clearly contradicting the first Maxwell’s equation. In the previous paragraphs, these effects are discussed in detail: the Van Vleuten effect $\nabla \times H = j$, by $j = 0, \nabla \times H \neq 0$, the Chetaev effect ($j_z = 0, \sigma \neq 0, E_z \neq 0$).

Hence, to find the explanation to such an unusual behavior of natural electromagnetic fields on the Earth, one should pay attention to the fact that the Earth is a cosmic body, for which hydromagnetic effects of magnetic fields, observed in the cosmos, are certain to be intrinsic [5].

The Earth’s electromagnetic field and the Earth as a whole as a cosmic object are characterized by hydromagnetic effects in the magnetic field with only exception that a non-force toroidal magnetic field is generated in the Earth’s atmosphere by the toroidal electric currents either in the Earth’s ionosphere, the sources of S_q -variations, or the electric currents flowing around the solid core in the zone F of the liquid core [10]. In this case, the above-mentioned effects are everywhere due to the non-potential non-force magnetic field H_T . According to $\nabla \times H_T = H_p$ this magnetic field does not generate electric currents thus it exists in the practically non-conducting Earth’s atmosphere and measured along with the poloidal force magnetic field H_p . The poloidal non-force electric field E_p is also present in the Earth’s atmosphere thus explaining its appearance in the Chetaev effect, being a part of the second non-force modification of the electromagnetic field of variations existing in the Earth’s atmosphere H_p, E_p is the non-force modification of the Earth’s electromagnetic field H_p, E_p are the force modifications. These modifications on regular boundaries are characterized by the following boundary conditions:

$$H_p^1 - H_p^2|_{r=R} = 0, \quad H_T^1 - H_T^2|_{r=R} = 0, \quad E_T^1 - E_T^2|_{r=R} = 0, \quad E_{Tn} = 0, \quad E_{pt}^1 - E_{pt}^2|_{r=R} = 0, \quad E_{pn}^1 = \frac{\sigma}{\sigma_1} E_{pn}^2. \tag{175}$$

In this case, the formulas for a two-module sounding of the Earth by the surface variation field can be written down in the following way:

$$Z^{MT} = \frac{i E_\theta^{MT}}{i H_\phi^{MT}}, \quad Z^{MT} = \frac{i E_\phi^{MT}}{i H_\theta^{MT}}, \quad Z^{ET} = \frac{E_r^i}{i H_\theta^{ET}}, \quad Z^{ET} = \frac{E_r^i}{i H_\phi^{ET}}, \tag{176}$$

$$\rho_k(\omega) = \frac{1}{\omega\mu} |Z^{MT} \cdot Z^{ET}| = \frac{1}{\omega\mu} Z_0^2.$$

Here i denotes belonging of fields to the internal sources, Z_0 is the impedance of

The electrically homogeneous Earth E_r^i is the recovered inductive part of the vertical electric field. The result of applying formulas (176) to experimental data are shown in table 3.

Table 3 shows that the account of the non-force part of the magnetic field of long-period quiet solar-daily variations (S_q -variations) observed in the atmosphere essentially smoothest values of the depths up to the Earth’s conducting layer at these temporal frequencies. This is the very manifestation of the non-force electromagnetic field in the experiment with natural electromagnetic fields.

An algorithm of separation of the variable non-force electromagnetic fields from the data observed on a sphere

Let inside a sphere and outside it there be sources of the variable harmonic electromagnetic field $e^{-i\omega t}$. Then the equation for the vector potential (73) for $t > 0$ is decomposed into two:

$$\Delta A^i + \bar{\alpha}^2 A^i = j_i^{CT}, \quad \Delta A^e + \bar{\alpha}^2 A^e = j_e^{CT}. \tag{177}$$

The solutions to these equations in the air have the form:

$$A^i(p) = \frac{1}{4\pi} \int_w j_i^{CT}(q) \frac{e^{-i\bar{\alpha}R(p,q)}}{R(p,q)} dw_q, \quad r \geq R_0; A^e(q) = \frac{1}{4\pi} \int_G j_e^{CT}(p) \frac{e^{i\bar{\alpha}R(p,q)}}{R(p,q)} dw_p, \quad r \leq R_0 + h. \tag{178}$$



Table 3:

Station	Coordinate system		Harmonic					Specific resistance (average), OMM	Depth, km
			1	2	3	4	5		
Leningrad	30,05	30,70	45	35	23	7	67	24	336
			22	9	5	38	3		
Moscow	34,52	37,32	73	46	10	1	222	64	555
			14	10	4	263	4		
Sverdlovsk	33,27	61,07	61	23	28	26	33	23	329
			26	2	3	20	15		
Kazan	34,17	48,85	70	52	25	26	74	31	381
			17	5	4	31	12		
Kiev	39,28	30,30	39	56	6	2	49	25	343
			13	11	6	67	6		
Pleshchenitsy	45,50	27,90	17	77	5	2	19	22	322
			14	11	10	61	10		
Lvov	40,10	23,73	27	120	5	4	20	25	343
			28	8	16	7	22		
Odessa	43,22	30,90	32	57	6	2	43	25	343
			11	12	6	80	5		
Tbilisi	47,92	44,70	35	17	10	74	39	20	307
			8	6	3	3	6		
Average								29	362

Here p is the point outside the sphere, q is the point inside the sphere, h is the height up to the external source, $j_i^{CT}(q)$ are the electric currents in the sphere, $j_e^{CT}(p)$ are the electric currents outside the sphere, R_0 and is the radius of the sphere.

The first integral represents the potential of the inner sources. It is analytical at all the points p for $r \geq R_0$. At the inner points of the sphere W for $R \rightarrow 0$ there is a specific feature of the form $1/R$ that is excluded by a proper choice of the Bessel spherical function of a semi-integer index tending to zero in zero. This will correspond to the physical matter, because the sources of many variations, for example, of the Earth's magnetic field, are damping with depth due to the influence of the skin effect, as it is an induced field of the external origin. At infinity, the integral provides the fulfilment of the radiation mode for the fields of internal sources. The second integral (178) represents the potential of external sources. It is analytical at all the points q except for $r \leq R_0 + h$, those where $R = 0$. At the latter, the potential possesses a peculiarity of the form $1/R$, which can be excluded by an appropriate selection of the Bessel function. Being specific at infinity, this integral can contribute to providing a specified growth of the field when approaching an external source. As the integral in question is employed in a limited domain, the peculiarity arising at infinity does not directly affect the calculation of the field between W and G .

By analogy with conventional decompositions of the function $1/R$ (77) [50], it is necessary to carry out decompositions of the fundamental solutions $\exp(\pm i\bar{\alpha} R) / R$ in terms of the spherical functions. It is clear that these decompositions due to the symmetry must differ from the Gauss decompositions only by the law of a change in the spherical coordinates r and r' , according to the physics of sources. The fulfilment of the condition of transferring the new decompositions to the Gauss decompositions, respectively, for the fields of external and internal sources for $\bar{\alpha} \rightarrow 0$ is also of importance.

Thus, let us write down decompositions of the functions needed using as radial ones the Bessel spherical functions in the Morse definition:

$$\begin{aligned} \exp(-i\bar{\alpha} R) / R &= \sum_{n=1}^{\infty} \sum_{m=0}^n \bar{c}_n^m \cos m\varphi \cos m\varphi' P_n^m(\cos \theta) P_n^m(\cos \theta') K_{n+1/2} \left(\frac{\alpha r}{R_0} \right) I_{n+1/2} \left(\frac{\alpha r'}{R_0} \right) + \\ \bar{c}_n^m \sin m\varphi \sin m\varphi' P_n^m(\cos \theta) P_n^m(\cos \theta') K_{n+1/2} \left(\frac{\alpha r}{R_0} \right) I_{n+1/2} \left(\frac{\alpha r'}{R_0} \right), \quad r \geq R_0. \end{aligned} \tag{179}$$

Similarly, for the functions with a positive exponent

$$\begin{aligned} \exp(i\bar{\alpha} R) / R &= \sum_{n=1}^{\infty} \sum_{m=0}^n \bar{c}_n^m \cos m\varphi \cos m\varphi' P_n^m(\cos \theta) P_n^m(\cos \theta') I_{n+1/2} \left(\frac{\alpha r}{R_0} \right) K_{n+1/2} \left(\frac{\alpha r'}{R_0} \right) + \\ \bar{c}_n^m \sin m\varphi \sin m\varphi' P_n^m(\cos \theta) P_n^m(\cos \theta') I_{n+1/2} \left(\frac{\alpha r}{R_0} \right) K_{n+1/2} \left(\frac{\alpha r'}{R_0} \right), \quad r \leq R_0 + h. \end{aligned} \tag{180}$$



In formulas (179) and (180), the coefficient \bar{c}_n^m means the number of combinations from n in terms of m . If the wave number α tends to zero, then due to the asymptotic behavior of the Bessel spherical functions with small arguments, the products of these functions of the first and second kinds yield a required ratio of the radii, and the expressions on the whole transfer to the Gauss decompositions for the function $1/R$.

Decomposition (179) is employed in the integration over the domain W , therefore the functions of the primed coordinates, it includes, exclude this peculiarity in zero. The functions with the unprimed coordinates do not possess this peculiarity because the decomposition with respect to them is used only for $r \geq R_0$.

Expansion (180) is exploited in the integration over the domain G , therefore the functions of the primed coordinates used for the integration exclude this peculiarity at infinity. The functions of the unprimed coordinates are specified for $r \leq R_0 + h$; therefore, their peculiarity at infinity is not valid: in zero, they tend to zero.

The convergence of decompositions (179) and (180) for $r = R_0$, is not worse than that of the Fourier series [20], which converge absolutely and uniformly, hence the substitution of these series into integrals (178) and changing places of integration and summation are possible. Let us make use of such a possibility without loss in generality.

In the rectangular coordinate system fixed at the center of a sphere, integrals (178) can be decomposed to components along the coordinate axes:

$$\begin{aligned}
 A_x^i(p) &= \frac{1}{4\pi} \int_W j_{ix}^{CT}(q) \frac{e^{-i\bar{\alpha} R(p,q)}}{R(p,q)} dw_q, A_y^i(p) = \frac{1}{4\pi} \int_W j_{iy}^{CT}(q) \frac{e^{-i\bar{\alpha} R(p,q)}}{R(p,q)} dw_q, A_z^i(p) = \frac{1}{4\pi} \int_W j_{iz}^{CT}(q) \frac{e^{-i\bar{\alpha} R(p,q)}}{R(p,q)} dw_q, \quad r \geq R_0, \\
 A_x^e(q) &= \frac{1}{4\pi} \int_G j_{ex}^{CT}(p) \frac{e^{i\bar{\alpha} R(p,q)}}{R(p,q)} dw_p, A_y^e(q) = \frac{1}{4\pi} \int_G j_{ey}^{CT}(p) \frac{e^{i\bar{\alpha} R(p,q)}}{R(p,q)} dw_p, A_z^e(q) = \frac{1}{4\pi} \int_G j_{ez}^{CT}(p) \frac{e^{i\bar{\alpha} R(p,q)}}{R(p,q)} dw_p, \quad r \leq R_0 + h.
 \end{aligned}
 \tag{181}$$

Now it is necessary to substitute decompositions (170) and (180) into (181) and to collect in integrals the functions of the primed coordinates. This will make possible to denote integrals by constants. For the constant internal sources, the following representations hold:

$$\begin{aligned}
 \rho_n^m &= \frac{\bar{c}_n^m}{4\pi} \int_W j_{ix}^{CT}(q) \cos m\varphi' P_n^m(\cos\theta') I_{n+1/2}\left(\frac{\alpha r'}{R_0}\right) dw', \rho_n^m = \frac{\bar{c}_n^m}{4\pi} \int_W j_{ix}^{CT}(q) \sin m\varphi' P_n^m(\cos\theta') I_{n+1/2}\left(\frac{\alpha r'}{R_0}\right) dw', \\
 \mu_n^m &= \frac{\bar{c}_n^m}{4\pi} \int_W j_{iy}^{CT}(q) \cos m\varphi' P_n^m(\cos\theta') I_{n+1/2}\left(\frac{\alpha r'}{R_0}\right) dw', \nu_n^m = \frac{\bar{c}_n^m}{4\pi} \int_W j_{iy}^{CT}(q) \sin m\varphi' P_n^m(\cos\theta') I_{n+1/2}\left(\frac{\alpha r'}{R_0}\right) dw', \\
 u_n^m &= \frac{\bar{c}_n^m}{4\pi} \int_W j_{iz}^{CT}(q) \cos m\varphi' P_n^m(\cos\theta') I_{n+1/2}\left(\frac{\alpha r'}{R_0}\right) dw', v_n^m = \frac{\bar{c}_n^m}{4\pi} \int_W j_{iz}^{CT}(q) \sin m\varphi' P_n^m(\cos\theta') I_{n+1/2}\left(\frac{\alpha r'}{R_0}\right) dw'.
 \end{aligned}
 \tag{182}$$

For arbitrary constant external sources, it is needed to introduce similar representations:

$$\begin{aligned}
 a_n^m &= \frac{\bar{c}_n^m}{4\pi} \int_G j_{ex}^{CT}(p) \cos m\varphi' P_n^m(\cos\theta') K_{n+1/2}\left(\frac{\alpha r'}{R_0}\right) dw', b_n^m = \frac{\bar{c}_n^m}{4\pi} \int_G j_{ex}^{CT}(p) \sin m\varphi' P_n^m(\cos\theta') K_{n+1/2}\left(\frac{\alpha r'}{R_0}\right) dw', \\
 c_n^m &= \frac{\bar{c}_n^m}{4\pi} \int_G j_{ey}^{CT}(p) \cos m\varphi' P_n^m(\cos\theta') K_{n+1/2}\left(\frac{\alpha r'}{R_0}\right) dw', d_n^m = \frac{\bar{c}_n^m}{4\pi} \int_G j_{ey}^{CT}(p) \sin m\varphi' P_n^m(\cos\theta') K_{n+1/2}\left(\frac{\alpha r'}{R_0}\right) dw', \\
 e_n^m &= \frac{\bar{c}_n^m}{4\pi} \int_G j_{ez}^{CT}(p) \cos m\varphi' P_n^m(\cos\theta') K_{n+1/2}\left(\frac{\alpha r'}{R_0}\right) dw', f_n^m = \frac{\bar{c}_n^m}{4\pi} \int_G j_{ez}^{CT}(p) \sin m\varphi' P_n^m(\cos\theta') K_{n+1/2}\left(\frac{\alpha r'}{R_0}\right) dw'.
 \end{aligned}
 \tag{183}$$

With allowance for the notations in (182) and (183) as well as for the formulas of transferring the rectangular components to the spherical ones (99), by way of substituting decompositions (170) and (180) into (181), it appears possible to obtain decompositions for the potentials of internal and external sources:

$$r \geq R_0.$$

$$\begin{aligned}
 A_\theta^i(p) &= \sum_{n=1}^{\infty} \sum_{m=0}^n [(\rho_n^m \cos m\varphi + \nu_n^m \sin m\varphi) \cos\theta \cos\varphi + (\mu_n^m \cos m\varphi + v_n^m \sin m\varphi) \cos\theta \cos\varphi - \\
 &\quad (u_n^m \cos m\varphi + v_n^m \sin m\varphi) \sin\theta] P_n^m(\cos\theta) K_{n+1/2}\left(\frac{\alpha r}{R_0}\right),
 \end{aligned}$$



$$A_{\varphi}^i(p) = \sum_{n=1}^{\infty} \sum_{m=0}^n [-(\alpha_n^m \cos m\varphi + \rho_n^m \sin m\varphi) \sin \varphi + (\mu_n^m \cos m\varphi + \nu_n^m \sin m\varphi) \cos \varphi] \times P_n^m(\cos \theta) K_{n+1/2} \left(\frac{\alpha r}{R_0} \right), \tag{184}$$

$$A_r^i(p) = \sum_{n=1}^{\infty} \sum_{m=0}^n [(\alpha_n^m \cos m\varphi + \rho_n^m \sin m\varphi) \sin \theta \cos \varphi + (\mu_n^m \cos m\varphi + \nu_n^m \sin m\varphi) \sin \theta \sin \varphi + (u_n^m \cos m\varphi + v_n^m \sin m\varphi) \cos \theta] P_n^m(\cos \theta) K_{n+1/2} \left(\frac{\alpha r}{R_0} \right), r \leq R_0 + h$$

$$A_{\theta}^e(q) = \sum_{n=1}^{\infty} \sum_{m=0}^n [(a_n^m \cos m\varphi + b_n^m \sin m\varphi) \cos \theta \cos \varphi + (c_n^m \cos m\varphi + d_n^m \sin m\varphi) \cos \theta \cos \varphi - (e_n^m \cos m\varphi + f_n^m \sin m\varphi) \sin \theta] P_n^m(\cos \theta) I_{n+1/2} \left(\frac{\alpha r}{R_0} \right),$$

$$A_{\varphi}^e(q) = \sum_{n=1}^{\infty} \sum_{m=0}^n [-(\alpha_n^m \cos m\varphi + b_n^m \sin m\varphi) \sin \varphi + (c_n^m \cos m\varphi + d_n^m \sin m\varphi) \cos \varphi] \times P_n^m(\cos \theta) I_{n+1/2} \left(\frac{\alpha r}{R_0} \right),$$

$$A_r^e(q) = \sum_{n=1}^{\infty} \sum_{m=0}^n [(a_n^m \cos m\varphi + b_n^m \sin m\varphi) \sin \theta \cos \varphi + (c_n^m \cos m\varphi + d_n^m \sin m\varphi) \sin \theta \sin \varphi + (e_n^m \cos m\varphi + f_n^m \sin m\varphi) \cos \theta] P_n^m(\cos \theta) I_{n+1/2} \left(\frac{\alpha r}{R_0} \right),$$

The analysis of decompositions of the potentials of internal and external sources (184) reveals that with this approach all the three components of a potential both of internal and external sources are expressed via the same coefficients that are integrals of the respective components of the current density, the latter generating both the poloidal and the toroidal parts of the observed field. The obtained decompositions of the potentials contain twelve types that are subject to determining constant coefficients. To define them, a more detailed information about the observed field, i.e. at a greater number of points, is needed. Below it will be possible to make certain that a disadvantage in the number of points provides an essential advantage as concerns measuring the required field components. In this case, it is sufficient to measure two components of the magnetic field: one vertical and one tangential for recovering all magnetic and all electric components of the field to separate the fields from the external and internal sources, and this is proved by the respective theorem.

Today, in the geophysical practice this fact is of principal importance because most of the world stations are measuring only magnetic components of the field.

For obtaining decompositions of the electromagnetic field of internal sources, it is necessary to substitute the first three components of the potential from (184) into (11) and (24). As a result, we arrive at the following:

$$H_{p\varphi}^i = \sum_{n=1}^{\infty} \sum_{m=0}^n [(\alpha_n^m \cos m\varphi + \rho_n^m \sin m\varphi) \sin \varphi - (\mu_n^m \cos m\varphi + \nu_n^m \sin m\varphi) \cos \varphi] \times P_n^m(\cos \theta) \left(\frac{n-1/2}{r} K_{n+1/2} \left(\frac{\alpha r}{R_0} \right) - \frac{\alpha}{R_0} K_{n-1/2} \left(\frac{\alpha r}{R_0} \right) \right),$$

$$H_{p\theta}^i = \sum_{n=1}^{\infty} \sum_{m=0}^n [(\alpha_n^m \cos m\varphi + \rho_n^m \sin m\varphi) \cos \theta \cos \varphi + (\mu_n^m \cos m\varphi + \nu_n^m \sin m\varphi) \cos \theta \sin \varphi - (u_n^m \cos m\varphi + v_n^m \sin m\varphi) \sin \theta] P_n^m(\cos \theta) \left(\frac{n-1/2}{r} K_{n+1/2} \left(\frac{\alpha r}{R_0} \right) - \frac{\alpha}{R_0} K_{n-1/2} \left(\frac{\alpha r}{R_0} \right) \right),$$

$$H_{pr}^i = \sum_{n=1}^{\infty} \sum_{m=0}^n \left[\alpha_n^m \left(\cos m\varphi \sin \varphi \frac{\partial P_n^m(\cos \theta)}{\partial \theta} - m \sin m\varphi \cos \varphi \operatorname{ctg} \theta P_n^m(\cos \theta) \right) + \rho_n^m \left(\sin m\varphi \sin \varphi \frac{\partial P_n^m(\cos \theta)}{\partial \theta} + m \cos m\varphi \cos \varphi \operatorname{ctg} \theta P_n^m(\cos \theta) \right) - \mu_n^m \left(\cos m\varphi \cos \varphi \frac{\partial P_n^m(\cos \theta)}{\partial \theta} + m \sin m\varphi \sin \varphi \operatorname{ctg} \theta P_n^m(\cos \theta) \right) - \nu_n^m \left(\sin m\varphi \cos \varphi \frac{\partial P_n^m(\cos \theta)}{\partial \theta} - m \cos m\varphi \sin \varphi \operatorname{ctg} \theta P_n^m(\cos \theta) \right) \right] \tag{185}$$



$$v_n^m \left(\sin m\varphi \cos \varphi \frac{\partial P_n^m(\cos \theta)}{\partial \theta} - m \cos m\varphi \sin \varphi \operatorname{ctg} \theta P_n^m(\cos \theta) \right) - (v_n^m \cos m\varphi - u_n^m \sin m\varphi) m P_n^m(\cos \theta) \frac{1}{r} K_{n+1/2} \left(\frac{\alpha r}{R_0} \right),$$

$$E_{T\theta}^i = -i\omega\mu_0 \sum_{n=1}^{\infty} \sum_{m=0}^n [(\alpha_n^m \cos m\varphi + \rho_n^m \sin m\varphi) \cos \theta \cos \varphi + (\mu_n^m \cos m\varphi + \nu_n^m \sin m\varphi) \cos \theta \sin \varphi -$$

$$(u_n^m \cos m\varphi + v_n^m \sin m\varphi) \sin \theta] P_n^m(\cos \theta) K_{n+1/2} \left(\frac{\alpha r}{R_0} \right), E_{P\varphi}^i = i\omega\mu_0 \sum_{n=1}^{\infty} \sum_{m=0}^n [(\alpha_n^m \cos m\varphi + \rho_n^m \sin m\varphi) \sin \varphi -$$

$$(\mu_n^m \cos m\varphi + \nu_n^m \sin m\varphi) \cos \varphi] P_n^m(\cos \theta) K_{n+1/2} \left(\frac{\alpha r}{R_0} \right),$$

The electric field of the internal sources type has the following decompositions:

$$H_{T\theta}^i = \sum_{n=1}^{\infty} \sum_{m=0}^n [-\alpha_n^m (m \sin m\varphi \cos \varphi + \cos m\varphi \sin \varphi) + \rho_n^m (m \cos m\varphi \cos \varphi - \sin m\varphi \sin \varphi) - \mu_n^m (m \sin m\varphi \sin \varphi - \cos m\varphi \cos \varphi) + \nu_n^m (m \cos m\varphi \sin \varphi + \sin m\varphi \cos \varphi) +$$

$$(v_n^m \cos m\varphi - u_n^m \sin m\varphi) m \operatorname{ctg} \theta] P_n^m(\cos \theta) \frac{1}{r} K_{n+1/2} \left(\frac{\alpha r}{R_0} \right), H_{T\varphi}^i = -\sum_{n=1}^{\infty} \sum_{m=0}^n \left[\alpha_n^m \cos m\varphi \cos \varphi \left(\cos \theta P_n^m(\cos \theta) + \sin \theta \frac{\partial P_n^m(\cos \theta)}{\partial \theta} \right) + \right.$$

$$\rho_n^m \sin m\varphi \cos \varphi \left(\cos \theta P_n^m(\cos \theta) + \sin \theta \frac{\partial P_n^m(\cos \theta)}{\partial \theta} \right) + \mu_n^m \cos m\varphi \sin \varphi \left(\cos \theta P_n^m(\cos \theta) + \sin \theta \frac{\partial P_n^m(\cos \theta)}{\partial \theta} \right) +$$

$$\nu_n^m \sin m\varphi \sin \varphi \left(\cos \theta P_n^m(\cos \theta) + \sin \theta \frac{\partial P_n^m(\cos \theta)}{\partial \theta} \right) + u_n^m \cos m\varphi \left(-\sin \theta P_n^m(\cos \theta) + \cos \theta \frac{\partial P_n^m(\cos \theta)}{\partial \theta} \right) + \quad (186)$$

$$v_n^m \sin m\varphi \left(-\sin \theta P_n^m(\cos \theta) + \cos \theta \frac{\partial P_n^m(\cos \theta)}{\partial \theta} \right) \left. \right] \frac{1}{r} K_{n+1/2} \left(\frac{\alpha r}{R_0} \right), E_{P\theta}^i = \frac{-1}{\sigma' r} \sum_{n=1}^{\infty} \sum_{m=0}^n \left[\alpha_n^m \cos m\varphi \cos \varphi \left(\cos \theta P_n^m(\cos \theta) + \sin \theta \frac{\partial P_n^m(\cos \theta)}{\partial \theta} \right) + \right.$$

$$\rho_n^m \sin m\varphi \cos \varphi \left(\cos \theta P_n^m(\cos \theta) + \sin \theta \frac{\partial P_n^m(\cos \theta)}{\partial \theta} \right) + \mu_n^m \cos m\varphi \sin \varphi \left(\cos \theta P_n^m(\cos \theta) + \sin \theta \frac{\partial P_n^m(\cos \theta)}{\partial \theta} \right) +$$

$$\nu_n^m \sin m\varphi \sin \varphi \left(\cos \theta P_n^m(\cos \theta) + \sin \theta \frac{\partial P_n^m(\cos \theta)}{\partial \theta} \right) + u_n^m \cos m\varphi \left(-\sin \theta P_n^m(\cos \theta) + \cos \theta \frac{\partial P_n^m(\cos \theta)}{\partial \theta} \right) +$$

$$v_n^m \sin m\varphi \left(-\sin \theta P_n^m(\cos \theta) + \cos \theta \frac{\partial P_n^m(\cos \theta)}{\partial \theta} \right) \left. \right] \times \left(\frac{n-3/2}{r} K_{n+1/2} \left(\frac{\alpha r}{R_0} \right) + \frac{\alpha}{R_0} K_{n-1/2} \left(\frac{\alpha r}{R_0} \right) \right),$$

$$E_{P\varphi}^i = \frac{-1}{\sigma' r} \sum_{n=1}^{\infty} \sum_{m=0}^n \left\{ [-\alpha_n^m (m \sin m\varphi \cos \varphi + \cos m\varphi \sin \varphi) + \rho_n^m (m \cos m\varphi \cos \varphi - \sin m\varphi \sin \varphi) - \right.$$

$$\mu_n^m (m \sin m\varphi \sin \varphi - \cos m\varphi \cos \varphi) + \nu_n^m (m \cos m\varphi \sin \varphi + \sin m\varphi \cos \varphi) \left. \right] P_n^m(\cos \theta) -$$

$$(-v_n^m \cos m\varphi + u_n^m \sin m\varphi) m \operatorname{ctg} \theta P_n^m(\cos \theta) \left. \right\} \left(\frac{n-3/2}{r} K_{n+1/2} \left(\frac{\alpha r}{R_0} \right) + \frac{\alpha}{R_0} K_{n-1/2} \left(\frac{\alpha r}{R_0} \right) \right),$$

$$E_{Pr}^i = \frac{1}{\sigma' r} \sum_{n=1}^{\infty} \sum_{m=0}^n [(\alpha_n^m \cos m\varphi + \rho_n^m \sin m\varphi) \sin \theta \cos \varphi + (\mu_n^m \cos m\varphi + \nu_n^m \sin m\varphi) \sin \theta \sin \varphi +$$

$$(u_n^m \cos m\varphi + v_n^m \sin m\varphi) \cos \theta] P_n^m(\cos \theta) \times$$

$$\left[\left(-\bar{\alpha}^2 r^2 + n^2 - 9/4 + \frac{\alpha^2 r^2}{R_0^2} \right) \frac{1}{r} K_{n+1/2} \left(\frac{\alpha r}{R_0} \right) - \frac{\alpha}{R_0} K_{n-1/2} \left(\frac{\alpha r}{R_0} \right) \right].$$

The analysis of the latter formulas reveals that both types of the fields, i.e. toroidal and poloidal are expressed via the same coefficients. In this case, the decomposition coefficients (185) and (186) indicate to the fact that for restoring the whole electromagnetic field of toroidal and poloidal fields of internal sources it is sufficient to measure the vertical component of the magnetic field H_{Pr}^i . This considerably enhances the importance of Theorem 7 because with its help it is possible to solve the



problem of variable periodic electromagnetic fields. On the surface of a sphere, the electric poloidal field is potential at $r = R_0$. The inductive part of the radial component E_{Tr}^e is compensated.

The fields H_p^e and E_T^e from external sources in the decompositions are written down in the following way:

The field at $r \leq R_0 + h$...

$$\begin{aligned}
 H_{p\theta}^e &= \sum_{n=1}^{\infty} \sum_{m=0}^n [(a_n^m \cos m\varphi + b_n^m \sin m\varphi) \sin \varphi - (c_n^m \cos m\varphi + d_n^m \sin m\varphi) \cos \varphi] \times \\
 &P_n^m(\cos \theta) \left(-\frac{n-1/2}{r} I_{n+1/2} \left(\frac{\alpha r}{R_0} \right) + \frac{\alpha}{R_0} I_{n-1/2} \left(\frac{\alpha r}{R_0} \right) \right), \\
 H_{p\varphi}^e &= \sum_{n=1}^{\infty} \sum_{m=0}^n [(a_n^m \cos m\varphi + b_n^m \sin m\varphi) \cos \theta \cos \varphi + (c_n^m \cos m\varphi + d_n^m \sin m\varphi) \cos \theta \sin \varphi - \\
 &(e_n^m \cos m\varphi + f_n^m \sin m\varphi) \sin \theta] P_n^m(\cos \theta) \left(-\frac{n-1/2}{r} I_{n+1/2} \left(\frac{\alpha r}{R_0} \right) + \frac{\alpha}{R_0} I_{n-1/2} \left(\frac{\alpha r}{R_0} \right) \right), \\
 H_{Pr}^e &= \sum_{n=1}^{\infty} \sum_{m=0}^n \left[a_n^m \left(\cos m\varphi \sin \varphi \frac{\partial P_n^m(\cos \theta)}{\partial \theta} - m \sin m\varphi \cos \varphi \text{ctg} \theta P_n^m(\cos \theta) \right) + \right. \\
 &b_n^m \left(\sin m\varphi \sin \varphi \frac{\partial P_n^m(\cos \theta)}{\partial \theta} + m \cos m\varphi \cos \varphi \text{ctg} \theta P_n^m(\cos \theta) \right) - c_n^m \left(\cos m\varphi \cos \varphi \frac{\partial P_n^m(\cos \theta)}{\partial \theta} + m \sin m\varphi \sin \varphi \text{ctg} \theta P_n^m(\cos \theta) \right) - \\
 &d_n^m \left(\sin m\varphi \cos \varphi \frac{\partial P_n^m(\cos \theta)}{\partial \theta} - m \cos m\varphi \sin \varphi \text{ctg} \theta P_n^m(\cos \theta) \right) - (f_n^m \cos m\varphi - e_n^m \sin m\varphi) m P_n^m(\cos \theta) \left. \right] \frac{1}{r} I_{n+1/2} \left(\frac{\alpha r}{R_0} \right), \tag{187}
 \end{aligned}$$

$$\begin{aligned}
 E_{T\theta}^e &= -i\omega\mu_0 \sum_{n=1}^{\infty} \sum_{m=0}^n [(a_n^m \cos m\varphi + b_n^m \sin m\varphi) \cos \theta \cos \varphi + (c_n^m \cos m\varphi + d_n^m \sin m\varphi) \cos \theta \sin \varphi - \\
 &(e_n^m \cos m\varphi + f_n^m \sin m\varphi) \sin \theta] P_n^m(\cos \theta) I_{n+1/2} \left(\frac{\alpha r}{R_0} \right), E_{T\varphi}^e = i\omega\mu_0 \sum_{n=1}^{\infty} \sum_{m=0}^n [(a_n^m \cos m\varphi + b_n^m \sin m\varphi) \sin \varphi - \\
 &(c_n^m \cos m\varphi + d_n^m \sin m\varphi) \cos \varphi] P_n^m(\cos \theta) I_{n+1/2} \left(\frac{\alpha r}{R_0} \right),
 \end{aligned}$$

The external sources field is similarly calculated at $r \leq R_0 + h$:

$$\begin{aligned}
 H_{T\theta}^e &= \sum_{n=1}^{\infty} \sum_{m=0}^n [-a_n^m (m \sin m\varphi \cos \varphi + \cos m\varphi \sin \varphi) + b_n^m (m \cos m\varphi \cos \varphi - \sin m\varphi \sin \varphi) - \\
 &c_n^m (m \sin m\varphi \sin \varphi - \cos m\varphi \cos \varphi) + d_n^m (m \cos m\varphi \sin \varphi + \sin m\varphi \cos \varphi) - \\
 &(f_n^m \cos m\varphi - e_n^m \sin m\varphi) m \text{ctg} \theta] P_n^m(\cos \theta) \frac{1}{r} K_{n+1/2} \left(\frac{\alpha r}{R_0} \right), \\
 H_{T\varphi}^e &= -\sum_{n=1}^{\infty} \sum_{m=0}^n \left[a_n^m \cos m\varphi \cos \varphi \left(\cos \theta P_n^m(\cos \theta) + \sin \theta \frac{\partial P_n^m(\cos \theta)}{\partial \theta} \right) + b_n^m \sin m\varphi \cos \varphi \left(\cos \theta P_n^m(\cos \theta) + \sin \theta \frac{\partial P_n^m(\cos \theta)}{\partial \theta} \right) + \right. \\
 &c_n^m \cos m\varphi \sin \varphi \left(\cos \theta P_n^m(\cos \theta) + \sin \theta \frac{\partial P_n^m(\cos \theta)}{\partial \theta} \right) + d_n^m \sin m\varphi \sin \varphi \left(\cos \theta P_n^m(\cos \theta) + \sin \theta \frac{\partial P_n^m(\cos \theta)}{\partial \theta} \right) + e_n^m \cos m\varphi \left(-\sin \theta P_n^m(\cos \theta) + \cos \theta \frac{\partial P_n^m(\cos \theta)}{\partial \theta} \right) + \\
 &f_n^m \sin m\varphi \left(-\sin \theta P_n^m(\cos \theta) + \cos \theta \frac{\partial P_n^m(\cos \theta)}{\partial \theta} \right) \left. \right] \frac{1}{r} I_{n+1/2} \left(\frac{\alpha r}{R_0} \right), E_{r\theta}^e = \frac{-1}{\sigma' r} \sum_{n=1}^{\infty} \sum_{m=0}^n \left[a_n^m \cos m\varphi \cos \varphi \left(\cos \theta P_n^m(\cos \theta) + \sin \theta \frac{\partial P_n^m(\cos \theta)}{\partial \theta} \right) + \right. \\
 &f_n^m \sin m\varphi \left(-\sin \theta P_n^m(\cos \theta) + \cos \theta \frac{\partial P_n^m(\cos \theta)}{\partial \theta} \right) \left. \right] \frac{1}{r} I_{n+1/2} \left(\frac{\alpha r}{R_0} \right), E_{r\varphi}^e = \frac{-1}{\sigma' r} \sum_{n=1}^{\infty} \sum_{m=0}^n \left[a_n^m \cos m\varphi \cos \varphi \left(\cos \theta P_n^m(\cos \theta) + \sin \theta \frac{\partial P_n^m(\cos \theta)}{\partial \theta} \right) + \right. \tag{188}
 \end{aligned}$$



$$\begin{aligned}
 & d_n^m \sin m\varphi \sin \varphi \left(\cos \theta P_n^m(\cos \theta) + \sin \theta \frac{\partial P_n^m(\cos \theta)}{\partial \theta} \right) + e_n^m \cos m\varphi \left(-\sin \theta P_n^m(\cos \theta) + \cos \theta \frac{\partial P_n^m(\cos \theta)}{\partial \theta} \right) + \\
 & f_n^m \sin m\varphi \left(-\sin \theta P_n^m(\cos \theta) + \cos \theta \frac{\partial P_n^m(\cos \theta)}{\partial \theta} \right) \left] \times \left(\frac{n-3/2}{r} I_{n+1/2} \left(\frac{\alpha r}{R_0} \right) - \frac{\alpha}{R_0} I_{n-1/2} \left(\frac{\alpha r}{R_0} \right) \right), \\
 E_{P\varphi}^e &= \frac{-1}{\sigma' r} \sum_{n=1}^{\infty} \sum_{m=0}^n \left[-a_n^m (m \sin m\varphi \cos \varphi + \cos m\varphi \sin \varphi) + b_n^m (m \cos m\varphi \cos \varphi - \sin m\varphi \sin \varphi) - \right. \\
 & c_n^m (m \sin m\varphi \sin \varphi - \cos m\varphi \cos \varphi) + d_n^m (m \cos m\varphi \sin \varphi + \sin m\varphi \cos \varphi) - \\
 & \left. (-f_n^m \cos m\varphi + e_n^m \sin m\varphi) m \cot \theta \right] P_n^m(\cos \theta) \left(\frac{n-3/2}{r} I_{n+1/2} \left(\frac{\alpha r}{R_0} \right) - \frac{\alpha}{R_0} I_{n-1/2} \left(\frac{\alpha r}{R_0} \right) \right), \\
 E_{Pr}^e &= \frac{1}{\sigma' r} \sum_{n=1}^{\infty} \sum_{m=0}^n \left[(a_n^m \cos m\varphi + b_n^m \sin m\varphi) \sin \theta \cos \varphi + (c_n^m \cos m\varphi + d_n^m \sin m\varphi) \cos \theta \right] P_n^m(\cos \theta) + \\
 & (e_n^m \cos m\varphi + f_n^m \sin m\varphi) \cos \theta \left] P_n^m(\cos \theta) \times \left[\left(-\bar{\alpha}^2 r^2 + n^2 - 9/4 + \frac{\alpha^2 r^2}{R_0^2} \right) \frac{1}{r} K_{n+1/2} \left(\frac{\alpha r}{R_0} \right) - \frac{\alpha}{R_0} K_{n-1/2} \left(\frac{\alpha r}{R_0} \right) \right].
 \end{aligned}$$

The field of external sources is also expressed via the same coefficients. The electric field is completely poloidal; the inductive part of the radial component of the electric field on the Earth's surface by $r = R_0$ is compensated because of $\bar{\alpha}^2 R_0^2 = \alpha^2$.

The summarized field is obtained by superposing the fields of internal and external sources. As a result, we have the equations separating unknown coefficients:

$$\begin{cases}
 \left\{ \begin{aligned}
 & a_n^m \frac{1}{r} K_{n+1/2} \left(\frac{\alpha r}{R_0} \right) + a_n^m \frac{1}{r} I_{n+1/2} \left(\frac{\alpha r}{R_0} \right) = i_n^m, \\
 & -a_n^m \frac{\alpha}{R_0} K_{n-1/2} \left(\frac{\alpha r}{R_0} \right) + a_n^m \frac{\alpha}{R_0} I_{n-1/2} \left(\frac{\alpha r}{R_0} \right) = \bar{i}_n^m;
 \end{aligned} \right. \\
 \left\{ \begin{aligned}
 & \rho_n^m \frac{1}{r} K_{n+1/2} \left(\frac{\alpha r}{R_0} \right) + b_n^m \frac{1}{r} I_{n+1/2} \left(\frac{\alpha r}{R_0} \right) = j_n^m, \\
 & -\rho_n^m \frac{\alpha}{R_0} K_{n-1/2} \left(\frac{\alpha r}{R_0} \right) + b_n^m \frac{\alpha}{R_0} I_{n-1/2} \left(\frac{\alpha r}{R_0} \right) = \bar{j}_n^m;
 \end{aligned} \right. \\
 \left\{ \begin{aligned}
 & \mu_n^m \frac{1}{r} K_{n+1/2} \left(\frac{\alpha r}{R_0} \right) + c_n^m \frac{1}{r} I_{n+1/2} \left(\frac{\alpha r}{R_0} \right) = k_n^m, \\
 & -\mu_n^m \frac{\alpha}{R_0} K_{n-1/2} \left(\frac{\alpha r}{R_0} \right) + c_n^m \frac{\alpha}{R_0} I_{n-1/2} \left(\frac{\alpha r}{R_0} \right) = \bar{k}_n^m;
 \end{aligned} \right. \\
 \left\{ \begin{aligned}
 & v_n^m \frac{1}{r} K_{n+1/2} \left(\frac{\alpha r}{R_0} \right) + d_n^m \frac{1}{r} I_{n+1/2} \left(\frac{\alpha r}{R_0} \right) = l_n^m, \\
 & -v_n^m \frac{\alpha}{R_0} K_{n-1/2} \left(\frac{\alpha r}{R_0} \right) + d_n^m \frac{\alpha}{R_0} I_{n-1/2} \left(\frac{\alpha r}{R_0} \right) = \bar{l}_n^m;
 \end{aligned} \right. \\
 \left\{ \begin{aligned}
 & u_n^m \frac{1}{r} K_{n+1/2} \left(\frac{\alpha r}{R_0} \right) + e_n^m \frac{1}{r} I_{n+1/2} \left(\frac{\alpha r}{R_0} \right) = q_n^m, \\
 & -u_n^m \frac{\alpha}{R_0} K_{n-1/2} \left(\frac{\alpha r}{R_0} \right) + e_n^m \frac{\alpha}{R_0} I_{n-1/2} \left(\frac{\alpha r}{R_0} \right) = \bar{q}_n^m;
 \end{aligned} \right.
 \end{cases} \tag{189}$$



$$\begin{cases} v_n^m \frac{1}{r} K_{n+1/2} \left(\frac{a r}{R_0} \right) + f_n^m \frac{1}{r} I_{n+1/2} \left(\frac{a r}{R_0} \right) = p_n^m, \\ -v_n^m \frac{a}{R_0} K_{n-1/2} \left(\frac{a r}{R_0} \right) + f_n^m \frac{a}{R_0} I_{n-1/2} \left(\frac{a r}{R_0} \right) = \bar{p}_n^m; \end{cases}$$

The summarized field of the poloidal field on the Earth's surface at $r = R_0$ looks like:

$$\begin{aligned} H_{P\theta} &= \sum_{n=1}^{\infty} \sum_{m=0}^n [(\bar{i}_n^m - (n-1/2)i_n^m) \cos m\varphi \sin \varphi + (\bar{j}_n^m - (n-1/2)j_n^m) \sin m\varphi \sin \varphi - \\ &(\bar{k}_n^m - (n-1/2)k_n^m) \cos m\varphi \cos \varphi - (\bar{l}_n^m - (n-1/2)l_n^m) \sin m\varphi \cos \varphi] P_n^m(\cos \theta), \\ H_{P\varphi} &= \sum_{n=1}^{\infty} \sum_{m=0}^n [(\bar{i}_n^m - (n-1/2)i_n^m) \cos m\varphi \cos \varphi \cos \theta + (\bar{j}_n^m - (n-1/2)j_n^m) \sin m\varphi \cos \varphi \cos \theta + \\ &(\bar{k}_n^m - (n-1/2)k_n^m) \cos m\varphi \sin \varphi \cos \theta + (\bar{l}_n^m - (n-1/2)l_n^m) \sin m\varphi \sin \varphi \cos \theta - \\ &(\bar{q}_n^m - (n-1/2)q_n^m) \cos m\varphi \sin \theta - (\bar{p}_n^m - (n-1/2)p_n^m) \sin m\varphi \sin \theta] P_n^m(\cos \theta), \\ H_{Pr} &= \sum_{n=1}^{\infty} \sum_{m=0}^n i_n^m \left(\cos m\varphi \sin \varphi \frac{\partial P_n^m(\cos \theta)}{\partial \theta} - m \sin m\varphi \cos \varphi \text{ctg} \theta P_n^m(\cos \theta) \right) + \\ &j_n^m \left(\sin m\varphi \sin \varphi \frac{\partial P_n^m(\cos \theta)}{\partial \theta} + m \cos m\varphi \cos \varphi \text{ctg} \theta P_n^m(\cos \theta) \right) - k_n^m \left(\cos m\varphi \cos \varphi \frac{\partial P_n^m(\cos \theta)}{\partial \theta} + m \sin m\varphi \sin \varphi \text{ctg} \theta P_n^m(\cos \theta) \right) - \\ &l_n^m \left(\sin m\varphi \cos \varphi \frac{\partial P_n^m(\cos \theta)}{\partial \theta} - m \cos m\varphi \sin \varphi \text{ctg} \theta P_n^m(\cos \theta) \right) - (p_n^m \cos m\varphi - q_n^m \sin m\varphi) m P_n^m(\cos \theta), \\ E_{T\theta} &= -i\omega\mu_0 R_0 \sum_{n=1}^{\infty} \sum_{m=0}^n (i_n^m \cos m\varphi \cos \varphi \cos \theta + j_n^m \sin m\varphi \cos \varphi \cos \theta + k_n^m \cos m\varphi \sin \varphi \cos \theta + l_n^m \sin m\varphi \sin \varphi \cos \theta - \\ &q_n^m \cos m\varphi \sin \theta - p_n^m \sin m\varphi \sin \theta) P_n^m(\cos \theta), E_{T\varphi} = i\omega\mu_0 R_0 \sum_{n=1}^{\infty} \sum_{m=0}^n (i_n^m \cos m\varphi \sin \varphi + j_n^m \sin m\varphi \sin \varphi - \\ &k_n^m \cos m\varphi \cos \varphi - l_n^m \sin m\varphi \cos \varphi) P_n^m(\cos \theta). \end{aligned} \tag{190}$$

The summarized toroidal field on the surface of a sphere at $r = R_0$ is of the form:

$$\begin{aligned} H_{T\theta} &= \sum_{n=1}^{\infty} \sum_{m=0}^n [-i_n^m (m \sin m\varphi \cos \varphi + \cos m\varphi \sin \varphi) + j_n^m (m \cos m\varphi \cos \varphi - \sin m\varphi \sin \varphi) - \\ &k_n^m (m \sin m\varphi \sin \varphi - \cos m\varphi \cos \varphi) + l_n^m (m \cos m\varphi \sin \varphi + \sin m\varphi \cos \varphi) - \\ &j_n^m \sin m\varphi \cos \varphi \left(\cos \theta P_n^m(\cos \theta) + \sin \theta \frac{\partial P_n^m(\cos \theta)}{\partial \theta} \right) + k_n^m \cos m\varphi \sin \varphi \left(\cos \theta P_n^m(\cos \theta) + \sin \theta \frac{\partial P_n^m(\cos \theta)}{\partial \theta} \right) + \\ &l_n^m \sin m\varphi \sin \varphi \left(\cos \theta P_n^m(\cos \theta) + \sin \theta \frac{\partial P_n^m(\cos \theta)}{\partial \theta} \right) + q_n^m \cos m\varphi \left(-\sin \theta P_n^m(\cos \theta) + \cos \theta \frac{\partial P_n^m(\cos \theta)}{\partial \theta} \right) + \\ &p_n^m \sin m\varphi \left(-\sin \theta P_n^m(\cos \theta) + \cos \theta \frac{\partial P_n^m(\cos \theta)}{\partial \theta} \right)], \\ E_{P\theta} &= \frac{1}{\sigma'_\zeta R_0} \sum_{n=1}^{\infty} \sum_{m=0}^n [(\bar{i}_n^m - (n-3/2)i_n^m) \cos m\varphi \cos \varphi \left(\cos \theta P_n^m(\cos \theta) + \sin \theta \frac{\partial P_n^m(\cos \theta)}{\partial \theta} \right) + \end{aligned} \tag{191}$$



$$\begin{aligned}
 & (\bar{j}_n^m - (n - 3/2)j_n^m) \sin m\varphi \cos \varphi \left(\cos \theta P_n^m(\cos \theta) + \sin \theta \frac{\partial P_n^m(\cos \theta)}{\partial \theta} \right) + \\
 & (\bar{k}_n^m - (n - 3/2)k_n^m) \cos m\varphi \sin \varphi \left(\cos \theta P_n^m(\cos \theta) + \sin \theta \frac{\partial P_n^m(\cos \theta)}{\partial \theta} \right) + \\
 & (\bar{l}_n^m - (n - 3/2)l_n^m) \sin m\varphi \sin \varphi \left(\cos \theta P_n^m(\cos \theta) + \sin \theta \frac{\partial P_n^m(\cos \theta)}{\partial \theta} \right) + \\
 & (\bar{q}_n^m - (n - 3/2)q_n^m) \cos m\varphi \left(-\sin \theta P_n^m(\cos \theta) + \cos \theta \frac{\partial P_n^m(\cos \theta)}{\partial \theta} \right) + \\
 & (\bar{p}_n^m - (n - 3/2)p_n^m) \sin m\varphi \left(-\sin \theta P_n^m(\cos \theta) + \cos \theta \frac{\partial P_n^m(\cos \theta)}{\partial \theta} \right) \Big],
 \end{aligned}$$

$$E_{P\varphi} = \frac{1}{\sigma'_c R_0} \sum_{n=1}^{\infty} \sum_{m=0}^n [-(\bar{i}_n^m - (n - 3/2)i_n^m)(m \sin m\varphi \cos \varphi + \cos m\varphi \sin \varphi) +$$

$$(\bar{j}_n^m - (n - 3/2)j_n^m)(m \cos m\varphi \cos \varphi - \sin m\varphi \sin \varphi) -$$

$$(\bar{k}_n^m - (n - 3/2)k_n^m)(m \sin m\varphi \sin \varphi - \cos m\varphi \cos \varphi) +$$

$$(\bar{l}_n^m - (n - 3/2)l_n^m)(m \cos m\varphi \sin \varphi + \sin m\varphi \cos \varphi) -$$

$$(\bar{q}_n^m - (n - 3/2)q_n^m)m \sin m\varphi \cot \theta +$$

$$(\bar{p}_n^m - (n - 3/2)p_n^m)m \cos m\varphi \cot \theta] P_n^m(\cos \theta),$$

$$E_{Pr} = \frac{1}{\sigma' R_0} \sum_{n=1}^{\infty} \sum_{m=0}^n [(\bar{i}_n^m + (n^2 - 9/4)i_n^m) \cos m\varphi \sin \theta \cos \varphi +$$

$$(\bar{j}_n^m + (n^2 - 9/4)j_n^m) \sin m\varphi \cos \varphi \sin \theta +$$

$$(\bar{k}_n^m + (n^2 - 9/4)k_n^m) \cos m\varphi \sin \varphi \sin \theta +$$

$$(\bar{l}_n^m + (n^2 - 9/4)l_n^m) \sin m\varphi \sin \varphi \sin \theta +$$

$$(\bar{q}_n^m + (n^2 - 9/4)q_n^m) \cos m\varphi \cos \theta +$$

$$(\bar{p}_n^m + (n^2 - 9/4)p_n^m) \sin m\varphi \cos \theta] P_n^m(\cos \theta).$$

The summarized field of variations that is observed on the surface of a sphere is obtained by superposing the fields of the magnetic and electric types. In superposing, it is necessary to take into account the two important circumstances.

The first one is in that in practice (at stations) the component H_θ is observed with the inverse sign (as usual, a measuring device is directed to the North) and the stress values in the observed components are given in Nano T.

The second circumstance is in that the intensity of electric components is measured in V/m. Therefore, the above-obtained formulas must be multiplied by the coefficient $10^{-2}/4\pi$. It will be recalled that all the formulas have been obtained for one temporal harmonic. The observed field contains an infinite variety of such temporal harmonics, thus before making the spherical analysis – for which the formulas were obtained – one should perform the Fourier harmonic analysis. The description of the latter is omitted because of its relative simplicity.

Thus, components of the summarized observed field of the global electromagnetic variations on a sphere have the following expansions:



$$\begin{aligned}
 H_\theta &= -\sum_{n=1}^{\infty} \sum_{m=0}^n [\bar{i}_n^m \cos m\varphi \sin \varphi + \bar{j}_n^m \sin m\varphi \sin \varphi - \bar{k}_n^m \cos m\varphi \cos \varphi - \bar{l}_n^m \sin m\varphi \cos \varphi - \\
 & i_n^m (m \sin m\varphi \cos \varphi + (n+1/2) \cos m\varphi \sin \varphi) + \\
 & j_n^m (m \cos m\varphi \cos \varphi - (n+1/2) \sin m\varphi \sin \varphi) + \\
 & k_n^m (m \sin m\varphi \sin \varphi - (n+1/2) \cos m\varphi \cos \varphi) + \\
 & l_n^m (m \cos m\varphi \sin \varphi + (n+1/2) \sin m\varphi \cos \varphi) + \\
 & (p_n^m \cos m\varphi - q_n^m \sin m\varphi) m c t g \theta] P_n^m(\cos \theta), \\
 H_\varphi &= \sum_{n=1}^{\infty} \sum_{m=0}^n [\bar{i}_n^m \cos m\varphi \cos \theta \cos \varphi + \bar{j}_n^m \sin m\varphi \cos \theta \cos \varphi + \bar{k}_n^m \cos m\varphi \cos \theta \sin \varphi \\
 & + \bar{l}_n^m \sin m\varphi \sin \theta \cos \theta - \\
 & (\bar{p}_n^m \sin m\varphi + \bar{q}_n^m \cos m\varphi) \sin \theta] P_n^m(\cos \theta) - \\
 & i_n^m \left(\sin \theta \frac{\partial P_n^m(\cos \theta)}{\partial \theta} + (n+1/2) \cos \theta P_n^m(\cos \theta) \right) \cos m\varphi \cos \varphi - \\
 & j_n^m \left(\sin \theta \frac{\partial P_n^m(\cos \theta)}{\partial \theta} + (n+1/2) \cos \theta P_n^m(\cos \theta) \right) \sin m\varphi \cos \varphi - \\
 & k_n^m \left(\sin \theta \frac{\partial P_n^m(\cos \theta)}{\partial \theta} + (n+1/2) \cos \theta P_n^m(\cos \theta) \right) \cos m\varphi \sin \varphi - \\
 & l_n^m \left(\sin \theta \frac{\partial P_n^m(\cos \theta)}{\partial \theta} + (n+1/2) \cos \theta P_n^m(\cos \theta) \right) \sin m\varphi \sin \varphi - \\
 & p_n^m \left(\cos \theta \frac{\partial P_n^m(\cos \theta)}{\partial \theta} - (n+1/2) \sin \theta P_n^m(\cos \theta) \right) \sin m\varphi - \\
 & q_n^m \left(\cos \theta \frac{\partial P_n^m(\cos \theta)}{\partial \theta} - (n+1/2) \sin \theta P_n^m(\cos \theta) \right) \cos m\varphi, \\
 H_r &= \sum_{n=1}^{\infty} \sum_{m=0}^n i_n^m \left(\cos m\varphi \sin \varphi \frac{\partial P_n^m(\cos \theta)}{\partial \theta} - m \sin m\varphi \cos \varphi c t g \theta P_n^m(\cos \theta) \right) + \\
 & j_n^m \left(\sin m\varphi \sin \varphi \frac{\partial P_n^m(\cos \theta)}{\partial \theta} + m \cos m\varphi \cos \varphi c t g \theta P_n^m(\cos \theta) \right) - \\
 & k_n^m \left(\cos m\varphi \cos \varphi \frac{\partial P_n^m(\cos \theta)}{\partial \theta} + m \sin m\varphi \sin \varphi c t g \theta P_n^m(\cos \theta) \right) - \\
 & l_n^m \left(\sin m\varphi \cos \varphi \frac{\partial P_n^m(\cos \theta)}{\partial \theta} - m \cos m\varphi \sin \varphi c t g \theta P_n^m(\cos \theta) \right) - \\
 & (p_n^m \cos m\varphi - q_n^m \sin m\varphi) m P_n^m(\cos \theta), \\
 E_\theta &= \frac{10^{-2}}{4\pi\sigma'_c R_0} \sum_{n=1}^{\infty} \sum_{m=0}^n \left[-i_n^m \left((\varrho^2 + n - 3/2) \cos \theta P_n^m(\cos \theta) + (n - 3/2) \sin \theta \frac{\partial P_n^m(\cos \theta)}{\partial \theta} \right) + \right.
 \end{aligned}$$



$$\begin{aligned} & \bar{i}_n^m \left(\cos \theta P_n^m(\cos \theta) + \sin \theta \frac{\partial P_n^m(\cos \theta)}{\partial \theta} \right) \Big] \cos m\varphi \cos \varphi + \left[-j_n^m \left((\alpha^2 + n - 3/2) \cos \theta P_n^m(\cos \theta) + (n - 3/2) \sin \theta \frac{\partial P_n^m(\cos \theta)}{\partial \theta} \right) + \right. \\ & \bar{j}_n^m \left(\cos \theta P_n^m(\cos \theta) + \sin \theta \frac{\partial P_n^m(\cos \theta)}{\partial \theta} \right) \Big] \sin m\varphi \cos \varphi + \left[-k_n^m \left((\alpha^2 + n - 3/2) \cos \theta P_n^m(\cos \theta) + (n - 3/2) \sin \theta \frac{\partial P_n^m(\cos \theta)}{\partial \theta} \right) + \right. \\ & \bar{k}_n^m \left(\cos \theta P_n^m(\cos \theta) + \sin \theta \frac{\partial P_n^m(\cos \theta)}{\partial \theta} \right) \Big] \cos m\varphi \sin \varphi + \left[-l_n^m \left((\alpha^2 + n - 3/2) \cos \theta P_n^m(\cos \theta) + (n - 3/2) \sin \theta \frac{\partial P_n^m(\cos \theta)}{\partial \theta} \right) + \right. \\ & \bar{l}_n^m \left(\cos \theta P_n^m(\cos \theta) + \sin \theta \frac{\partial P_n^m(\cos \theta)}{\partial \theta} \right) \Big] \sin m\varphi \sin \varphi + \left[q_n^m \left((\alpha^2 + n - 3/2) \sin \theta P_n^m(\cos \theta) - (n - 3/2) \cos \theta \frac{\partial P_n^m(\cos \theta)}{\partial \theta} \right) + \right. \\ & \bar{q}_n^m \left(-\sin \theta P_n^m(\cos \theta) + \cos \theta \frac{\partial P_n^m(\cos \theta)}{\partial \theta} \right) \Big] \cos m\varphi + \left[p_n^m \left((\alpha^2 + n - 3/2) \sin \theta P_n^m(\cos \theta) - (n - 3/2) \cos \theta \frac{\partial P_n^m(\cos \theta)}{\partial \theta} \right) + \right. \\ & \bar{p}_n^m \left(-\sin \theta P_n^m(\cos \theta) + \cos \theta \frac{\partial P_n^m(\cos \theta)}{\partial \theta} \right) \Big] \sin m\varphi, \end{aligned}$$

$$E_\varphi = \frac{10^{-2}}{4\pi\sigma'_c R_0} \sum_{n=1}^{\infty} \sum_{m=0}^n [i_n^m ((n - 3/2)m \sin m\varphi \cos \varphi + (\alpha^2 + n - 3/2) \cos m\varphi \sin \varphi) +$$

$$\bar{i}_n^m (m \sin m\varphi \cos \varphi + \cos m\varphi \sin \varphi) + \bar{j}_n^m (m \cos m\varphi \cos \varphi - \sin m\varphi \sin \varphi) + j_n^m (-(n - 3/2)m \cos m\varphi \cos \varphi + (\alpha^2 + n - 3/2) \sin m\varphi \sin \varphi) -$$

$$\bar{k}_n^m (m \sin m\varphi \sin \varphi - \cos m\varphi \cos \varphi) - k_n^m (-(n - 3/2)m \sin m\varphi \sin \varphi + (\alpha^2 + n - 3/2) \cos m\varphi \cos \varphi) +$$

$$\bar{l}_n^m (m \cos m\varphi \sin \varphi + \sin m\varphi \cos \varphi) - l_n^m ((n - 3/2)m \cos m\varphi \sin \varphi + (\alpha^2 + n - 3/2) \sin m\varphi \cos \varphi) - (\bar{q}_n^m - (n - 3/2)q_n^m)m \sin m\varphi \cos \theta +$$

$$(\bar{p}_n^m - (n - 3/2)p_n^m)m \cos m\varphi \sin \theta] P_n^m(\cos \theta),$$

$$E_r = \frac{10^{-2}}{4\pi\sigma'_R R_0} \sum_{n=1}^{\infty} \sum_{m=0}^n [(\bar{i}_n^m + (n^2 - 9/4)i_n^m) \cos m\varphi \sin \theta \cos \varphi + (\bar{j}_n^m + (n^2 - 9/4)j_n^m) \sin m\varphi \cos \varphi \sin \theta +$$

$$(\bar{k}_n^m + (n^2 - 9/4)k_n^m) \cos m\varphi \sin \varphi \sin \theta + (\bar{l}_n^m + (n^2 - 9/4)l_n^m) \sin m\varphi \sin \varphi \sin \theta +$$

$$(\bar{q}_n^m + (n^2 - 9/4)q_n^m) \cos m\varphi \cos \theta + (\bar{p}_n^m + (n^2 - 9/4)p_n^m) \sin m\varphi \cos \theta] P_n^m(\cos \theta)$$

The analysis of the above decompositions shows that all the components of the observed electromagnetic field have the same unknown constants. As a rule, three magnetic components are measured at a worldwide network of stations, a few of them measuring the toroidal electric components. Hence, the spherical analysis must cover all the available information about components of the field. In this case, it appears possible to decrease the effect of random measurement errors in the inversion of the basic matrix.

According to (192), the electric components of the field of global electromagnetic variations may not be measured. They can be calculated by means of the results of the spherical analysis of magnetic components only. This is of importance because the measurements are aimed at recording only magnetic components.

According to (192) the vertical electric component of the field on the Earth's surface is potential. Its inductive part is compensated by this potential. The analysis of (189) and (192) allows the formulation of the following theorem for a variable electromagnetic field:

Theorem 12

The full separation of observed electromagnetic fields to toroidal and poloidal as well as to external and internal fields in them is uniquely resolvable when the vertical and one of horizontal components of the magnetic field are known.

The algorithm of solving the full separation problem is in the following. A certain number (up to a given upper limit of summation n in (192)) of the coefficients with a dash and without it is calculated by the measured at the worldwide network of stations magnetic components of the field of variations by the spherical analysis technique. Then with these coefficients, the synthesis of the summarized field is carried out in terms of (192). If at each point the synthesis of the field slightly differs from that observed (by the given ε), then the number of the coefficients obtained by the analysis made is considered to be sufficient for presenting the observed field on the sphere.



After that, equations (189) are solved, and using the coefficients obtained, the toroidal and poloidal fields from external and internal sources are synthesized poloidal and toroidal field. They can be calculated by formulas (190) and (191) in the summarized field with the same coefficients with textures and without trait, which were obtained by the spherical analysis technique.

According to Gauss and Schmidt, the spherical analysis method of the observation data for the calculation of coefficients is approximate. The approximation degree depends on rejecting infinite sums of expansions (192) finishing on a preliminarily specified number n . The value of a possible for such a rejection number n depends on the number of available observational points on the surface of the sphere. The larger is their number – up to the greater number n the easier a field can be expanded. The sufficiency for interpolating the field of a chosen number n is defined by the method of comparison of the observed field and its synthesis.

The Algorithm of recovering the variable toroidal electric currents on a sphere generating non-force electromagnetic fields

The sources of geoelectromagnetic variations are simulated by the results of the spherical analysis of their field observed on the spherical surface of a sphere (in the first approximation, the Earth is considered to be spherical). In this case, the full separation of fields of variations contributes to solving the simulation problem thus providing the isolation of a field of the external origin in both modifications. In the theory of current systems, the principle of modeling equivalent sources was introduced long ago. This principle is based on transferring from a magnetic field of external sources to a double layer of charges whose power was identified with the force of an equivalent current. The contours of the equivalent current force form a current system equivalent to that existing in nature. Numerous academic studies deal with investigations of the systems of currents.

However, in connection with the existence of a toroidal magnetic field it is needed to solve a number of new problems.

The first problem is in the development of physical grounds of the way of constructing a current system to be adequate to an observed field. It may be based on separation of two modifications of a field (toroidal and poloidal) and on the development of physically substantiated approach to transferring from an observed field to its source.

The second problem is in deducing all the necessary formulas suitable for the numerical calculation.

The third one is in applying the theory to a concrete material of observations and in elucidating the new features of sources whose existence is predetermined by the existence of a toroidal field that was not considered earlier in the theory.

When modeling the poloidal magnetic field sources it is necessary to take into account certain assumptions. First, the Earth is considered to be sphere-shaped, the electric currents, generating toroidal and poloidal magnetic fields – to be concentrated in the Ionosphere thin layer E at a height $h = 120$ km from the Earth.

Second, based on physical considerations and the fact that a toroidal field is excluded in advance, it follows that a thin layer, i.e. the supporter of the current system is spherically symmetric to the Earth, otherwise a toroidal field, which was excluded in advance, would appear. In this case, it is natural to assume that interaction of currents has occurred before separation of fields, that is why the poloidal field represents the final picture of the current distribution in a source.

The next important assumption is in that the surface, i.e. a supporter of current is supposed to be infinitely thin, and above and below it the whole surface is filled with the air with conductivity σ' or it is empty $\sigma' = 0$.

However, if the current concentrates on a thin surface, the magnetic field components tangential to it satisfy on this surface the boundary condition of the form:

$$j(p) = [n, (H^+(p) - H^-(p))]. \quad (193)$$

Here $H^+(p)$ is the magnetic field at the point p above the layer with current, $H^-(p)$

is the magnetic field at the point p under the layer with current, $j(p)$ is the surface current, n is the external normal. In the above statement, the medium properties above and below the layer with current are considered to be equal, therefore the magnetic field components will differ only in their sign. The decomposition coefficients of the field under and above the layer coincide on the layer. In order to make certain, let us consider a simple example. Let the conductivity above and below the layer be equal to zero $\sigma' = 0$, then it is possible to apply simplified decompositions for a poloidal field. The coefficients of these simplified decompositions are expressed via integrals. As an example, let us take one coefficient from the outer side of the surface:



$$a_n^m = \frac{\bar{c}_n^m}{4\pi\tilde{R}^{n+2}} \int_W r'^m j_{x'}^{CT}(x', y', z') \cos m\varphi' P_n^m(\cos \theta') dw' \tag{194}$$

Where W is the layer above the Earth \tilde{R} is the distance from the Earth's center up to the layer W . From the inner side of the layer, the corresponding coefficient will be of the form:

$$a_n^m = \frac{\bar{c}_n^m \tilde{R}^{n-1}}{4\pi} \int_W \frac{1}{r'^{m+1}} j_{x'}^{CT}(x', y', z') \cos m\varphi' P_n^m(\cos \theta') dw' \tag{195}$$

Here r' – is the radius. If the thickness of the layer tends to zero, then the radii are transformed as follows:

$$\tilde{R} = R_0 + h; \quad r' = R_0 + h, \tag{196}$$

Where R_0 – is the sphere radius, h – is the height to the surface with the current from the Earth's surface. In this case, in integrals (194) and (195), the steady volume current must be replaced by the surface current. The surface one must replace the volume integration. As a result, we come to:

$$a_n^m = \frac{\bar{c}_n^m}{4\pi(R_0 + h)^2} \int_{\Sigma} j_{x'}^{CT}(x', y', z') \cos m\varphi' P_n^m(\cos \theta') ds', \quad a_n^m = \frac{\bar{c}_n^m}{4\pi(R_0 + h)^2} \int_{\Sigma} j_{x'}^{CT}(x', y', z') \cos m\varphi' P_n^m(\cos \theta') ds' \tag{197}$$

Where Σ is the surface with current ds' is the surface element.

It is clear that in (197), the coefficients at different sides of an infinitely thin surface with current are described by the same expressions. Similar operations can also be made with the rest coefficients and to make certain that they coincide as well, i.e., really, in transferring a thin layer with electric current, the tangential components change only a sign, the coefficients at both sides of the layer with current being coincident. Thus, when constructing the formulas for the surface current density it is possible to make use of the decompositions of fields below the surface with current.

From the outer side of the surface with current, the tangential components will be of the form:

$$H_{P\theta}^+ = -\sum_{n=1}^{\infty} \sum_{m=0}^n [(a_n^m \cos m\varphi + b_n^m \sin m\varphi) \sin \varphi - (c_n^m \cos m\varphi + d_n^m \sin m\varphi) \cos \varphi] P_n^m(\cos \theta) \times \left(-\frac{n-1/2}{R_0+h} I_{n+1/2}(\alpha \frac{R_0+h}{R_0}) + \frac{\alpha}{R_0} I_{n-1/2}(\alpha \frac{R_0+h}{R_0}) \right), \tag{198}$$

$$H_{P\varphi}^+ = -\sum_{n=1}^{\infty} \sum_{m=0}^n [(a_n^m \cos m\varphi + b_n^m \sin m\varphi) \cos \theta \cos \varphi + (c_n^m \cos m\varphi + d_n^m \sin m\varphi) \cos \theta \sin \varphi - (e_n^m \cos m\varphi + f_n^m \sin m\varphi) \sin \theta] P_n^m(\cos \theta) \left(-\frac{n-1/2}{R_0+h} I_{n+1/2}(\alpha \frac{R_0+h}{R_0}) + \frac{\alpha}{R_0} I_{n-1/2}(\alpha \frac{R_0+h}{R_0}) \right),$$

From the inner side of the surface with electric current, the expressions for the tangential components of the magnetic field are written down in the following way:

$$H_{P\theta}^- = \sum_{n=1}^{\infty} \sum_{m=0}^n [(a_n^m \cos m\varphi + b_n^m \sin m\varphi) \sin \varphi - (c_n^m \cos m\varphi + d_n^m \sin m\varphi) \cos \varphi] P_n^m(\cos \theta) \times \left(-\frac{n-1/2}{R_0+h} I_{n+1/2}(\alpha \frac{R_0+h}{R_0}) + \frac{\alpha}{R_0} I_{n-1/2}(\alpha \frac{R_0+h}{R_0}) \right), \tag{199}$$

$$H_{P\varphi}^- = \sum_{n=1}^{\infty} \sum_{m=0}^n [(a_n^m \cos m\varphi + b_n^m \sin m\varphi) \cos \theta \cos \varphi + (c_n^m \cos m\varphi + d_n^m \sin m\varphi) \cos \theta \sin \varphi -$$



$$(e_n^m \cos m\varphi + f_n^m \sin m\varphi) \sin \theta] P_n^m(\cos \theta) \left(-\frac{n-1/2}{R_0+h} I_{n+1/2}(\alpha \frac{R_0+h}{R_0}) + \frac{\alpha}{R_0} I_{n-1/2}(\alpha \frac{R_0+h}{R_0}) \right)$$

Now expressions (198) and (199) are to be substituted into formula (193). In so doing, it is more convenient to write it in components:

$$j_\theta^i = H_{P\varphi}^+ - H_{P\varphi}^-; \quad j_\varphi^i = H_{P\theta}^+ - H_{P\theta}^- \tag{200}$$

For the radial function, it is possible to introduce the notation

$$\psi_n(\alpha, h) = \left(-\frac{n-1/2}{R_0+h} I_{n+1/2}(\alpha \frac{R_0+h}{R_0}) + \frac{\alpha}{R_0} I_{n-1/2}(\alpha \frac{R_0+h}{R_0}) \right) \tag{201}$$

For the calculation, it is required to introduce into the final formulas the factor $10^{-2}/4\pi$, transferring the values of coefficients obtained in Nano T to A/m . As it is required to investigate the behavior of the current systems in terms of time, it is suitable to reconstruct the dependence of the current density on time that was earlier everywhere omitted. With allowance for all the above-stated, the electric current components on the infinitely thin surface at a height h from the sphere will be of the form:

$$j_\theta^i = \frac{-10^{-2}}{2\pi} \sum_{k=-\infty}^{\infty} \sum_{n=1}^{\infty} \sum_{m=0}^n [(a_n^m \cos m\varphi + b_n^m \sin m\varphi) \cos \theta \cos \varphi + (c_n^m \cos m\varphi + d_n^m \sin m\varphi) \cos \theta \sin \varphi - (e_n^m \cos m\varphi + f_n^m \sin m\varphi) \sin \theta]_k \psi_n(\alpha, h) P_n^m(\cos \theta) e^{i\omega k t},$$

$$j_\varphi^i = \frac{10^{-2}}{2\pi} \sum_{k=-\infty}^{\infty} \sum_{n=1}^{\infty} \sum_{m=0}^n [(a_n^m \cos m\varphi + b_n^m \sin m\varphi) \sin \varphi - (c_n^m \cos m\varphi + d_n^m \sin m\varphi) \cos \varphi]_k P_n^m(\cos \theta) \psi_n(\alpha, h) e^{i\omega k t} \tag{202}$$

The surface current density components in (202) are of dimension in A/m thus allowing the construction of distributing the current density vectors on a specified surface. A set of such vectors constructed by a given instant of the world time represents a current system generating a poloidal field. The current system constructed using a poloidal field will be trivially without divergence because a toroidal field is preliminarily excluded. The choice of the world time for constructing the current systems is explained by a synchronous change in the variations in the unified world time [3]. The adequacy of a source to the observed field is ensured by formula (200) because the electric current is directly calculated by the field components without any transformations.

With the application program package developed, it is possible to calculate the current systems by a poloidal field. Figure 3 presents a current system of the field of variations S_q by 1958/1959. This system has been obtained by 6 o'clock world time.

The following is of importance. On the daily side, there are known current contours: the southern - with the clockwise rotation and the northern - in the counter-clockwise direction. The contours are divided by the eastern electric current that flows in the vicinity of the equator and corresponds to the known electro jet. The line connecting the centers of vortices on the daily side tends to the direction of the force lines of the MGF. This fact was not noted earlier. The night side similar to the dayside has northern and southern vortices but of the opposite rotation direction and separated by the current of the western direction. The line connecting the centers of the night vortices is also close to the direction of the MGF force lines. An important result is that during a day, the night vortices can move towards the morning or evening sides. Such a symmetric picture of current vortices of a magnetic type field has never been noted earlier. In our opinion, this is in agreement with the physics of sources and is adequate to the observed field.

Thus, the approach proposed to constructing a model of the poloidal field source has allowed the elucidation of a sufficiently simple morphological structure of the source of the solar-daily variations. The current variations system S is a set of the two symmetric on the day and on the night sides (or on the morning and evening sides) and oppositely rotating systems of currents separated by electric jet of the east and west directions, respectively. The source of variations S has none of the other contours in addition to those above-mentioned. The symmetric picture of the location of the current vortices corresponds to the morphology of the daily variations S observed on the Earth's surface and is in agreement with the electrodynamics of the phenomenon.

Thus, the method proposed for constructing a model for a source of a poloidal field made it possible to reveal a fairly simple morphological structure of the source of the solar-daily variations. The current system S_q of variations is a combination of two symmetric on the day and on the night sides (or on the morning and evening sides) and oppositely rotating systems of currents

separated by electro jets of the east and west directions, respectively. There are no other contours other than those mentioned above. The symmetric pattern of the location of current vortices corresponds to the morphology of the daily variations observed on the Earth's surface, and is consistent with the electrodynamics of the phenomenon.

Further, in the equatorial region, due to the analysis of the invisible part of the vertical electric field, electro jets with vertical influxes on the morning and evening sides of the day were detected. It is clear that these vertical currents can only be within the limits of the ionosphere, where there are horizontal and vertical conductivities. Nevertheless, the fact of the presence of injections is well traced by the anomalous behavior in the morning and evening hours of the induction part of the vertical electric field (Figure 6), which was reconstructed from the results of a spherical analysis of the magnetic components of the solar-daily variations.

The in-depth analysis of all the new facts arising after the separation of toroidal and poloidal fields in S_q variations and in each of them into the fields of external and internal sources allowed the author to propose his own model of the source S_q of variations, which, as it seems, substantially amplifies the well-known classical model of variations in the ionosphere (Figure 6).

The generation of such a current system of variations S_q , which is shown in figure 6, apparently, must depend on the winds at a height E of the ionosphere layer, plasma drift in it at the equator by a day to the west, at night to the east (the current flows in the opposite direction), stationary convection in the lower magnetosphere. The degree of contribution of one or another mechanism to generating regular currents S_q still has to be revealed. The mechanism of the appearance of the vertical current at the equator on the morning and evening sides of the day, which, as it is, is extremely interesting, seems completely unclear. Nevertheless, the fact of the appearance of vertical inflows at the equator seems to be indisputable.

Thus, studying the source only of variations S_q provided obtaining a number of new interesting facts. The facts of similar importance can be identified in the sources of all other types of variations, it is only necessary to apply decomposition (192) to their investigation, with allowance for all the electrodynamic information currently available on the global electromagnetic field of variations.

The algorithm for calculating electrodynamic parameters of a non-force magnetic field source in the Earth's core

In Section, dealing with natural sources of the Earth's non-force magnetic field, the distance to the source of the MGF and its main electrodynamic parameters is calculated. This section presents an algorithm for calculating these electrodynamic parameters.

The calculation of the Earth's toroidal and poloidal magnetic fields of the Earth in the zone F of the liquid core begins with the statement of the current source radius, calculated in Section 11, equal to 1437 km.

The magnetic moment magnitude of a toroidal magnetic field at this radius and at a radius of 1371 km (a radius of 1371 km is mentioned in the scientific literature) can be calculated by the formula:

$$H_{TF} \cdot R_F^3 = M_{TF}, \tag{203}$$

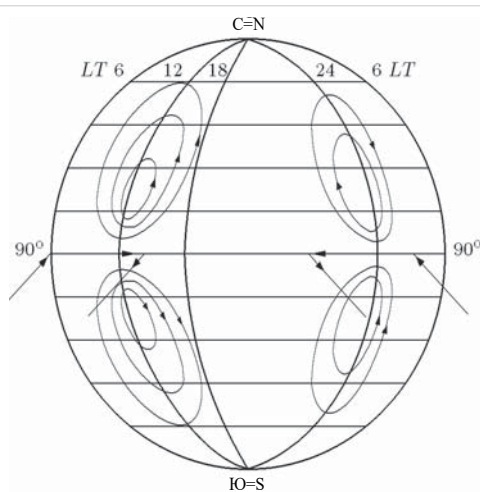


Figure 6: The external source of variations, simulated from toroidal non-force and poloidal force fields for MGY-1957/58 (LT- local time in hours).



Where H_{TF} is the intensity of the toroidal magnetic field in the zone F , M_{TF} is the magnetic moment, R_F is the radius of the zone F .

On the Earth's surface, the magnetic moment of the toroidal field is calculated by the formula:

$$H_T \cdot R_0^3 = M_T. \tag{204}$$

Since the magnetic moment of the MGF is constant, then comparing (203) and (204), we can determine the ratio of the magnetic fields in the zone in terms of the magnetic field on the surface:

$$|H_{TF}| = |H_T| \left(\frac{R_0}{R_F}\right)^3 = |H_T| \left(\frac{6371}{1437}\right)^3 \approx |H_T| \cdot 90 \Big|_{r=1437}, \quad |H_{TF}| = |H_T| \left(\frac{6371}{1371}\right)^3 = |H_T| \cdot 100 \Big|_{r=1371} \tag{205}$$

Thus, the toroidal field in the liquid core zone F with its radius known from the scientific literature, is 100 times greater than the intensity values on the Earth's surface and 90 times greater at a depth of the calculated distance to the source.

The absolute value of the toroidal field strength in the source with a radius of 1,437 km, with allowance for formula (205), is equal to:

$$|H_T| = |H_p| \cdot 0,06 = 3,1 \text{ Gs}$$

With a radius of 1371 we obtain:

$$|H_T| = |H_p| \cdot 0,06 = 3,6 \text{ Gs} \tag{206}$$

It can be assumed that in the zone of the liquid core the intensity of the Earth's toroidal magnetic field does not exceed 3-4 G_s .

The intensity of the poloidal magnetic field, calculated by the same method of comparing the magnetic moments on the Earth's surface and in the core zone F , gives the following values:

$$|H_p|_{1371} = 60 \text{ Гс}, \quad |H_p|_{1437} = 52,3 \text{ Gs} \tag{207}$$

The values H_p and H_T of magnetic fields at a depth will be further used in the calculation of the parameters of the electric current, i.e. the source of the MGF.

As is revealed higher, a toroidal magnetic field is present in the Earth's atmosphere. The spherical analysis of the MGF observed on the Earth's surface and the separation of the toroidal magnetic field from the poloidal one gives only 0.035 Gauss for $|H_T|$ on the Earth's surface. Using the property of continuity of the magnetic field, it is possible to calculate it in the source: formulas (205), (206). In this case, its intensity does not exceed 3-4 G_s .

However, a weak toroidal field is present on the Earth's surface and in its core, so its nature must be clarified. The author [10] has shown that to generate such a toroidal magnetic field in the Earth's atmosphere, the sphericity of the source, which is an electric current, is sufficient. The equation for the full current in the source is known:

$$-j^i = \nabla \nabla \cdot A - \nabla \times \nabla \times A \tag{208}$$

The components of the vector potential A , according to (31) and (32) are expressed in terms of a scalar function Q as follows:

$$A_\theta = \frac{\partial Q}{\sin \theta \partial \varphi}; \quad A_\varphi = -\frac{\partial Q}{\partial \theta}; \quad A_r = rQ \tag{209}$$

Here r, θ, ϕ are the spherical coordinates. The components of the toroidal field, by definition from (32), have the form:

$$-j_\theta^i = \frac{\partial^2 A_\theta}{\partial r^2} + \frac{2\partial A_\theta}{r\partial r} + \frac{1}{r^2 \sin^2 \theta} \frac{\partial^2 A_\theta}{\partial \varphi^2} + \frac{1}{r^2} \frac{\partial^2 A_\theta}{\partial \theta^2} - \frac{\cos \theta}{r^2 \sin \theta} \frac{\partial A_\theta}{\partial \theta} - \frac{A_\theta}{r^2 \sin^2 \theta} - 2 \frac{\cos \theta}{r^2 \sin^2 \theta} \frac{\partial A_\varphi}{\partial \varphi} + \frac{2\partial A_r}{r^2 \partial \theta}; \tag{210}$$

If we construct an equation for the full current on the axis of a spherical coordinate system fixed at the Earth's center, then we can obtain the following projections of the components of the electric current, including those in the source:

$$-j_\varphi^i = \frac{1}{r \sin \theta} \frac{\partial}{\partial \theta} \sin \theta \frac{\partial A_\varphi}{\partial \varphi} + \frac{1}{r^2 \sin \theta} \frac{\partial^2 A_\varphi}{\partial \varphi^2} + \frac{1}{r} \frac{\partial^2 r A_\varphi}{\partial r^2} + \frac{\cos \theta}{r^2 \sin^2 \theta} \frac{\partial A_\theta}{\partial \varphi} - \frac{\cos \theta}{r^2 \sin \theta} \frac{\partial A_\varphi}{\partial \varphi} + \frac{1}{r^2} \frac{\partial}{\partial \theta} \frac{1}{\sin \theta} \frac{\partial}{\partial \theta} \sin \theta A_\varphi - \frac{1}{r} \frac{\partial^2 A_\varphi}{\partial \theta \partial \varphi} + \frac{2}{r^2 \sin \theta} \frac{\partial A_r}{\partial \varphi}. \tag{211}$$



Here the expressions:

$$\frac{2\partial A_r}{r^2 \sin \theta \partial \varphi} = \frac{2}{r \sin \theta} \frac{\partial Q}{\partial \varphi} = \frac{2}{r} H_{T\theta}; \quad \frac{2\partial A_r}{r^2 \partial \theta} = \frac{2}{r} \frac{\partial Q}{\partial \theta} = -\frac{2}{r} H_{T\varphi}$$

With allowance for formulas (209) and (210), are just doubled components of the toroidal magnetic field, assigned to the current radius, which gives them the dimension of the current density. Thus, the spherical electric current with its spherical components always “generates” a toroidal magnetic field that appears on the Earth’s surface, according to the boundary conditions from (35), and is measured at the World Network of Magnetic Observatories with the help of magnetometers, which directly fix the intensity of the observed MGF.

In [10], the presence of H_p and H_r in the MGF for 1964 is proved. From this follows an unambiguous conclusion that the MGF is caused by the spherical electric current, the poloidal and toroidal magnetic fields being excited by this current, are present in the atmosphere and are contained in its measured values, including those in the data obtained at the World Network of Magnetic Observatories and in any other magneto metric measurements, with the exception of magnetic prospecting, in which magnetic masses are the source of the magnetic field.

The Earth’s rotation naturally brings about the rotation of charged particles if they are present in the liquid part of the core, namely, in the core zone F. To estimate the speed of rotation of charged particles in the liquid core, the estimates for a pair of equations are used [10]:

$$\rho \left[\frac{\partial \mathbf{U}}{\partial t} + (\mathbf{U} \text{grad}) \mathbf{U} + 2(\boldsymbol{\omega} \times \mathbf{U}) \right] = \nu \rho \Delta \mathbf{U} + \text{grad} P' + [\mathbf{j} \times \mathbf{B}] + \mathbf{f}; \quad \frac{\partial \mathbf{B}}{\partial t} = (\mathbf{B} \text{grad}) \mathbf{U} - (\mathbf{U} \text{grad}) \mathbf{B} - \eta \Delta \mathbf{B}, \tag{212}$$

where U is the linear flow velocity, B is the magnetic induction, j is the current density, ρ is the substance density, P' is the pressure minus the hydrostatic pressure, ν, η are the kinematic and magnetic viscosities, respectively, ω is the velocity vector of the angular rotation. Omitting the cumbersome intermediate expressions given in [10], we write down the final formula for the components of the linear flow velocity:

$$U_{\varphi}^{1,2} = \pm \left[\left(\frac{P'}{\rho} - gh \right) \frac{H_{\varphi}}{|\mathbf{H}|} \right]^{1/2} \mp 2L\omega_{\varphi}, \quad U_r^1 \approx -\frac{P'}{2L\rho\omega_{\varphi}} + 2L\omega_{\varphi}, \quad U_{\theta}^1 \approx \frac{P'}{2L\rho\omega_{\varphi}} - 2L\omega_{\varphi}. \tag{213}$$

If we substitute into formula (213) the values of the known parameters for the liquid core and the zone F equal to:

$$\nu = 10^3 \frac{m^2}{s} \quad \omega_{\varphi} = 7,3 \cdot 10^{-5} \frac{1}{s} \quad T = 1,8 \cdot 10^{15} \text{ s} \quad P = 2,445 \cdot 10^{12} \frac{G}{sm \times s^2} \quad \eta = 2,6 \frac{m^2}{s}$$

$$g = 226 \frac{sm}{s^2} \quad h = 4,9 \cdot 10^8 \text{ sm} \quad L = 2,9 \cdot 10^8 \text{ sm} \quad \frac{H_{\varphi}}{|\mathbf{H}|} = 0,0216, \quad \frac{H_r}{|\mathbf{H}|} = 0,8, \quad \frac{H_{\theta}}{|\mathbf{H}|} = 0,5,$$

Then the numerical estimate for the components of the absolute linear velocity of the flow takes the values:

$$U_{\varphi} \approx 50 \frac{m}{s}, \quad U_r, U_{\theta} \approx 10^{-4} \frac{m}{s}. \tag{214}$$

These values clearly indicate to the rotational motion of the flow. The other two components in (214) are “suppressed” by the rotation. The angular velocity of the rotation is calculated by the known formula and is:

$$\omega_{U_{\varphi}} = \frac{U_{\varphi}}{R_F} = 3,4 \cdot 10^{-5} \frac{1}{s} \tag{215}$$

This angular flow velocity is somewhat less than the angular velocity of the Earth’s rotation $\omega_{\varphi} = 7,3 \cdot 10^{-5} \frac{1}{s}$. This important circumstance allows, according to the principle of relativity, an electric field to exist in the stream. An observer directly involved in examining the uniformly rotating Earth does not “see” the electric field of a stream if the rotation of the stream coincides with the Earth’s rotation. Outstripping or delay in the flow is necessary. In our example, there is an obvious delay, which ensures the presence of an electric field in the stream. In addition, this directly confirms the presence of the electric current in the zone F of the Earth’s liquid core, whose electrodynamic parameters will be calculated below.

Studying the nature and intensity of the toroidal magnetic field in the liquid core, or more precisely, in the core zone F , where the MGF source is located, has clearly demonstrated that this field is due to the sphericity of the source, i.e. the electric current. Therefore, the question arises about the way of the appearance of electric current in the zone F of the liquid core. It is clear that



this is a stream of charged particles, most likely, judging by the direction of the MGF force lines, electrons directed by the Earth's rotation from west to east. The magnetic field has the north and south poles.

It is clear that there must be some kind of an external magnetic field that would provide a "seed" at the time instant when, for example, an induction electric current has appeared.

To calculate the value of the initial external field, it is necessary to know the Reynolds numbers: kinematic and magnetic [10]. The kinematic Reynolds number for the liquid core is selected at the level of 100–150 units, because these values determine the boundary between laminarity and turbulence of the flow in the liquid core [26]. The magnetic Reynolds numbers given here are units $10^3 \div 10^5$ do not prohibiting the occurrence of turbulence, possibly, in local temperature anomalies against the background of a common laminar flow of charged particles. Such an assumption, generally speaking, is a kind of compromise between the flow laminarity and local turbulence, which may occur, thus reflecting the age-related anomalies observed in the MGF. Anyway, the kinematic Reynolds number allows estimating the power, i.e. the width of the stream of charged particles, based on the relation:

$$R_c = \frac{U_\varphi \cdot l}{\nu}; \quad l = 150 \cdot 10^{-3} / 50 = 3 \cdot 10^{-3} \text{ m} \tag{216}$$

Where ν is the kinematic viscosity from (213).

Such a low flow velocity of about three kilometers is caused by a relatively small kinematic viscosity, which significantly narrows the flow, despite relatively a large kinematic Reynolds number, which, in turn, leads to "broadening" the flow intensity. The interaction of opposing tendencies stabilizes the flow resulting in its steady-state existence, confirmed by the stability of the MGF.

The known intensity (width) of a stream of charged particles allows us to estimate the magnetic Reynolds number Re_m by the formula:

$$Re_m = l \cdot \sigma_F \cdot \mu_0 \cdot U_\varphi = 3 \cdot 10^3 \cdot 5 \cdot 10^5 \cdot 4\pi \cdot 10^{-7} \cdot 50 = 9,42 \cdot 10^4, \tag{217}$$

Where σ_E is the conductivity in the core zone F .

Such a large magnetic Reynolds number allows one to neglect ohmic losses. In this case, the induction excitation will be determined only by the reactive component. Then the initial magnetic field "seed" can be calculated based on the formula:

$$\mathbf{H} = \mathbf{H}_0 \cdot Re_m; \quad |\mathbf{H}_0| = \frac{|\mathbf{H}|}{Re_m} = \frac{60}{9,42 \cdot 10^4} = 6,37 \cdot 10^{-4} \text{ G}_s, \quad |\mathbf{H}_0| \approx 64 \text{ nT } \text{Gs} \tag{218}$$

Such a small, in terms of intensity, "seed" field for induction could well have existed in the beginning of appearance of the MGF, on the one hand, and on the other hand, it also supports the MGF now due to the influence of the constant component of the solar magnetic field through the "solar wind". As long as there is the sun, there will be the MGF. Its resistance to external and internal influences is expressed by formula (213). The stability is attained at the expense of inverse proportionality between the flow velocity and the magnetic field strength. The demagnetization brings about an increase in the flow velocity, the amplification of the magnetic field leads to a drop in the flow velocity, which is then aligned with the Earth's stable rotation. The Earth's stable rotation is a guarantee of the stability of the MGF as a whole. The focusing of the Earth's poles is implemented by a weak toroidal magnetic field, according to the formula:

$$[\mathbf{H}_T \times \mathbf{H}_p] = H_{pr} H_{T\varphi} e_\theta - H_{p\varphi} H_{T\theta} e_r + (H_{T\theta} H_{p\varphi} - H_{T\varphi} H_{p\theta}) e_r \tag{219}$$

The maximum values of the poloidal field at the poles are amplified by the components of the toroidal magnetic field, "turning" on the force lines of the poloidal field, according to formula (8). This leads to the focusing effect of the GGP at the poles. In this model of the GGP source, a change in polarity in the GGP, about which geologists discuss, can only happen by changing the direction of the Earth's rotation to the opposite, on the one hand, and eliminating the focus of the GGP poles for some reason, on the other. Events for the Earth, such as planets, are improbable.

In order to estimate, based on the data obtained, the electrodynamic parameters of a source, it is necessary to preliminarily estimate the geometric parameters of the flow, namely, its cross-sectional area and the volume occupied by it. Because the source generates a toroidal magnetic field measured on the entire Earth's surface, we will assume that the source is distributed in a spherical layer from pole to pole with a thickness of three kilometers (216). Then the cross-sectional area of the half-layer will be equal to:



$$S_F = \frac{\pi}{2}(R_2^2 - R_1^2) = 13,5 \cdot 10^9 m^2 \quad (220)$$

Where $R_2 = 1,437 \cdot 10^6 m$; $R_1 = 1,434 \cdot 10^6 m$.

The volume of the layer in cubic meters will be equal to:

$$V_F = \frac{4}{3}\pi(R_2^3 - R_1^3) = 7,8 \cdot 10^{16} m^3 \quad (221)$$

Based on the equality of the magnetic moments, expressed through a magnetic field and through the strength of the current, according to the following formula

$$|H_F| \cdot R_F^3 = S_F \cdot I \quad (Am^2)$$

it appears possible to calculate the strength of the current in the source. It is equal to:

$$I = \frac{|H_F| \cdot R_F^3}{S_F} = \frac{60 \cdot 4\pi \cdot 10^{-3} \cdot (1,437)^3 \cdot 10^{18}}{13,5 \cdot 10^9} = 1,66 \cdot 10^8 A \quad (222)$$

Thus, the strength of current in the source is about 166 million amperes.

The current density in the source can be estimated as follows:

$$|j| = \frac{I}{S_F} = \frac{1,66 \cdot 10^8}{13,5 \cdot 10^9} = 1,23 \cdot 10^{-2} \quad A / m^2 \quad (223)$$

The number of particles per cubic meter in the source is estimated through the current density and the flow velocity:

$$j_\varphi = neU_\varphi \quad (224)$$

The amount of charge in a cubic meter is:

$$ne = \frac{j_\varphi}{U_\varphi} = \frac{1,23 \cdot 10^{-2}}{50} = 2,46 \cdot 10^{-4} \quad Q / m^3$$

Where Q is the amount of charge.

If we assume that in the source the electric current is generated by the flow of electrons, then the number of particles (electrons) will be equal to:

$$n = \frac{2,46 \cdot 10^{-4}}{1,6 \cdot 10^{-19}} \approx 15 \cdot 10^{14} \quad \text{Particles}' / m^3 \quad (225)$$

Here $e = 1,6 \cdot 10^{-19}$ is the electron charge.

The maximum conductivity of the liquid core is known [26]. It is of order $\sigma_F = 5 \cdot 10^5 \quad [\frac{Sm}{m}]$, and then the electric field can be estimated by the formula:

$$|E_F| = \frac{|j_F|}{\sigma_F} = \frac{1,23 \cdot 10^{-2}}{5 \cdot 10^5} = 2,46 \cdot 10^{-8} \quad V / m \quad (226)$$

Such an electric field is provided by the delay of the electron flux with respect to the angular velocity of the Earth's rotation.

The amount of charge in the layer is estimated by the amount of charge per cubic meter multiplied by the volume of the layer (221), namely:

$$neV_F = 2,46 \cdot 10^{-4} \cdot 7,8 \cdot 10^{16} = 1,92 \cdot 10^{13} \quad Q \cdot \quad (227)$$

The charge in the layer rotates with an angular velocity (215), so the current generated by it in one of the directions will be equal to half the charge multiplied by the angular velocity of the flow:



$$I = \frac{1}{2} neV_f \omega_{V_p} = 0,5 \cdot 1,92 \cdot 10^{13} \cdot 3,4 \cdot 10^{-5} = 3,26 \cdot 10^8 \text{ A} \quad (228)$$

Or $6 \cdot 10^8 \text{ A}$ for the full charge present in the layer.

These values of the current strength in order of magnitude coincide with the current strength calculated from the equality of the moments calculated by the magnetic field (222).

Thus, the electrodynamic parameters of the MGF source, which are the conduction electric current provided by the flow of free electrons in the liquid core zone *F*, excite the values of poloidal and toroidal magnetic fields observed on the Earth, (Figure 2). The electric current is supported by the Earth's stable rotation and insignificant induction seed to be set by the Sun's magnetic field and the interplanetary magnetic field. As long as the magnetic fields rather weak in the Earth's region exist, the stable Main Geomagnetic Field of the Earth will be stable. With its stability, the MGF has ensured the long-lasting evolution of the Earth's biosphere.

Conclusion

A full-scale analysis of the occurrence of non-force electromagnetic fields within the Earth in the technical physics and in the physics of a natural electromagnetic field, considered in the theoretical part of this monograph, has revealed that a new physical phenomenon is subject to physical and mathematical substantiation and is not contradictory to a slight refinement to the well-known Maxwell's equations. Also, it satisfies the well-known classical theorems by Helmholtz, Gauss-Schmidt, Cowling. It is confirmed by the well-known experiments in the course of the world magnetic surveys and earlier world geophysical years. It is manifested in physical-technical experiments with quantum particles, in tokamaks and capacitors. It allows overcoming the well-known skin effect and the discontinuous behavior of the depths in the process of super-deep sounding, etc.

The author hopes for understanding of the new physical problems revealed by him and the ways of their explanation and resolution.

References

- Chandrasekhar S. On force-free magnetic fields. Proceedings of the National Academy of Sciences of the United States of America. 1956; 42: 1–5. [PubMed: https://www.ncbi.nlm.nih.gov/pmc/articles/PMC534220/](https://www.ncbi.nlm.nih.gov/pmc/articles/PMC534220/)
- Van Vleuten A. Over de dagelijkse variatie van het Ardmagnetisme. Koninklijk Ned. Meteor. Instit. No. 102, Utrecht. 1917; 5–30.
- Benkova NP. Solar Diurnal variations of Terrestrial Magnetism. The Hydrometeorological service of USSR Transactions of Scientific Institutions. Terrestrial Magnetism. Series VI. L.-M.: 1941; 75.
- Aksenov VV. Toroidal field in the Earth's atmosphere. Novosibirsk. Russian Academy of Sciences Siberian Branch. 1997; 133.
- Parker EN. Cosmical Magnetic Fields. Clarendon Press Oxford. 1997; 1: 608; 2.
- Moffat HK. Generation of magnetic field in conducting medium. Cambridge University Press. 1978; 339.
- Aksenov VV. On three Kinds of Electrodynamics on the Earth and in Space. The Way of Science. 2017; 7: 8–15.
- Larmor J. How could a rotating body such as the Sun become a magnet. Rep Brit Assoc SCI. 1919; 60 –159.
- Aksenov VV. The Toroidal Decomposition of the Vector Potential of a Magnetic Field and its Applications. Moscow University Physics Bulletin Physics of Earth, Atmosphere and Hydrosphere. 2015; 70: 558–565.
- Aksenov VV. The Earth's Electromagnetic Field. – Novosibirsk. Inst. Of Math and Math. Geophysics. 2010; 268.
- Aksenov VV. On mutual generation of magnetic fields in tokamaks and its suppression. Russian Phy J. 2018; 61: 171-172.
- Aksenov VV. Non-Force and Force Electromagnetic Fields. Russian Phy J. 2016; 59: 319-327.
- Aksenov VV. Adaptation of Maxwell-Parker-Moffat Electrodynamics to Electromagnetic Fields Observed in the Earth's Atmosphere. Russian Phy J. 2017; 60: 389-398.
- Stratton J. Ad. Electromagnetic Theory. Mc. Graw-Hill Book Company. New York and London. 1941; 539.
- Marsh GE. Force-Free Magnetic Fields: Solution, Topology and Applications. Singapore: World Scientific Publishing Co. PTL. Ltd. 1966; 157.
- Cowling TG. Mgnethydrodynamics. John Willey and Sons. New York. 1957; 139.
- Yak Z, Rusmikin A, Socoloff D. Magnetic field in astrophysics. Gordon and Breach, New York. 1983; 483.
- Alfven H. Cosmical Electrodynamics. Oxford: University Press. 1950; 240.



19. Korn GA, Korn TM. *Mathematical Handbook for Scientist and Engineers Definitions, Theorems and Formulas for Reference and Review*. McGraw-Hill Book Company, INC, New York Toronto London. 1961; 720.
20. Tikhonov AN, Samarsky AA. *Equations of Mathematical Physics*. M.: Nauka. 1972; 735.
21. Gauss KF. *Allgemeine Theorie des Erdmagnetismus*. Werke. 1838-1839; T5, S. 119.
22. Gauss KF. *Allgemeine Lehrsätze in Beziehung auf die in verkehrten verhältnisse des Quadrats der Entfernung wirkenden Anziehung und Abstossungskräfte*. Werke. 1839-1840; T.4, S. 195.
23. Schmidt A. *Besitzt die tagliche erdmagnetische Schwankung in der Erdoberfläche ein Potential*. Physik. Zeitschrift. 1918; 19: 349–355.
24. Aksenov VV. *On Some Solenoidal Vector Fields in Spherical Domains*. Differential Equations. 2012; 48: 1042 – 1045.
25. Aksenov VV. *On Methodology and Methods of Applied Geomagnetism*. Geology and Rasvedka. 2016; 50–55.
26. Parkinson WD. *Introduction to Geomagnetism*. Scottish Academic Press. Edinburg and London. 1983; 520.
27. Yanovsky BM. *Telluric Magnetism*. Leningrad: GITTL. 1978; 591.
28. Gauss RF. *Isbrannie trudi po semnomu magnetizmu*. L.: Izd AN SSSR. 1952; 343.
29. Chetaev DN. *O structure polya korotkoperiodicheskoy geomagnitnoy variazii and magnitotelluricheskoy sondirovani*. Physics of the Earth. 1970; 52–55.
30. Sokolov DD, Stepanov PA, Frik PG. *Dinamo na puti ot astrofisischeskih modeley k laboratornomu experimentu*. UFN. 2014. 184: 313–335. [PubMed](#):
31. Aksenov VV. *Modeling of a Magnetic Field of Sources Localized within a sphere and beyond*. Mathematical Modeling. 2015; 27: 111–126.
32. Aksenov VV. *The Foundations of Geomagnetism*. Bulletin of the Novosibirsk Computing Center. Series: Mathematical Modeling in Geophysics. Special Issue: 15. 2012; 100.
33. Stern DP. *Representation of magnetic field in Space*. Rev. Geophys. 1976; 199 – 214.
34. Tikhonov AN, Arsenin B. Ya. *Metody resheniya nekorrektnih zadach*. Nauka. 1974; 223.
35. Aksenov VV. *Ob Istochnike Glavnogo Geomagnitnogo Polya*. Part 2. Geologiya and exploration. 2012; 54-60.
36. Moore EH. *General analysis*. Memoirs Phi Soc. 1935; 1-231.
37. Penrose R. *A Generalized inverse for matrices*. Proc. Camb. Phil. Soc. 1955; 51: 406–413.
38. Geller RJ, Jackson DD, Kagan YY, Mulagria F. *Earthquakes Cannot be Predicted*. Science. 1997; 1616–1617.
39. Alekseev AS, Aksenov VV. *Ob electricheskoy pole v ochagovoy zone zemletryasenii*. DAN. 2003; T. 392: 106–110.
40. Aksenov VV. *O modelirovani and assessment electromagnitnih and teplovih polei kak predvestnikov semletryasenii*. Geofisicheskii J. 2003; 25: 20–25.
41. Rabotnov JH, Lomakin EB. *Sootnosheniya teorii uprugosti dlya isotroprnogo raznomodulnogo tela*. AN SSSR. MTT. 1978; 29–34.
42. Lyahovskii VA, Myasnikov BG. *O povedenii uprugoi sredi s micro-narusheniyami*. Fizika Zemli. 1984; 71–75.
43. Ustundag B, Ozerden S. *Erthquake prediction using a new monopolar electric field probe*. European Seismological Congress (ESC 2002). Genoa. 2002.
44. Aaronov V, Bohm D. *Significance of Electromagnetic Potentials in the Quantum Theory*. Phys Rev. 1959; 115: 485–491.
45. Chirkov AG, Ageev AH. *O prirode effecta Aaronova-Bohma*. JTF. 2001; 71: 16–22.
46. Azizov EA. *Tokamaks from A.D. Sakharov to nowadays (the 60 year tokamak history)*. UFN. 2012; 182: 202–215.
47. Dyrdin VV, Elkin IS, Lozhkin KV, Sosnov FS. *Magnitnoe pole tokov smeshcheniya*. Vestnik of Kuzbass State Technicfl University. 2004; 5: 36–37.
48. Bullard EC. *The magnetic Field within the Earth*. Proc Roy Soc Lond. 1949; 433–453.
49. Rikitaki T. *Electromagnetism i Vnutrennee stroenie Zemli*. M.: Nauka. 1968; 236.
50. Aksenov VV. *Non-force electromagnetic field*. Int J Phy Res Applic. 2020; 20–45.